Johanna Aho

Rheological Characterization of Polymer Melts in Shear and Extension: Measurement Reliability and Data for Practical Processing

Tampere 2011

Johanna Aho

Rheological Characterization of Polymer Melts in Shear and Extension: Measurement Reliability and Data for Practical Processing

Thesis for the degree of Doctor of Science in Technology to be presented with due permission for public examination and criticism in Konetalo Building, Auditorium K1702, at Tampere University of Technology, on the 20th of May 2011, at 12 noon.

ABSTRACT

In order to manage the processing of polymers one needs to understand and be able to quantify the rheological phenomena occurring in complex flows of viscoelastic materials. Knowledge on rheological behavior of polymers is needed for setting the right process window, such as temperature and flow rate. In addition, rheological data is needed for process simulation, which is increasingly adapted as an important part of new process setup. Rheological properties of the polymer melt are of particular importance in flow modeling. Despite their importance, shortcuts in rheological measurements are often taken, which can lead to inaccurate or incorrect results.

The scope of the study was to add knowledge on the importance of different rheological properties of polymers regarding melt processing, to improve their measurement techniques and discuss possible errors in experiments. The focus of the work was on selected subjects important in polymer processing, the emphasis being on injection molding: measuring and modeling of polymer melt viscosity at low temperature and shear rates, pressure dependence of viscosity, and extensional viscosity. In addition, rheological data measured using an injection molding machine and a slit die were reported. Secondly, the correct way of performing experiments, measurement accuracy and correct data analysis were discussed in capillary rheometer measurements and uniaxial extensional viscosity measurements.

The results of Publication I showed that generalized Newtonian fluid (GNF) models, such as Carreau-Yasuda equation, were able to describe the viscosity function accurately for the studied amorphous polymers over the flow phases relevant in injection molding – high temperature and high shear rate, as in filling, or low shear rate and low temperature, as in packing. Dynamic oscillatory experiments at low temperatures showed a tendency towards an apparent 2nd Newtonian plateau at high angular frequencies.

Publication II discussed the correction of entrance pressure drop in capillary rheometry: an orifice die proved to offer a convenient short-cut for evaluating the entrance pressure drop, but the conical expansion area of the commercial design used here requires a correction for the additional pressure drop caused by the adhesion of the melt to the wall of the expansion area.

Publication III confirmed that the pressure dependence of viscosity, studied for several polymers, increases with increasing complexity. At lower temperatures, close to the glass transition temperature, the effect of pressure on viscosity is more pronounced, hence the test temperature must be taken into account when pressure dependence of viscosity for different polymers is compared.

Publication IV examined the experimental and analytical practice and errors in uniaxial extension experiments by Sentmanat extensional rheometer (SER). Modifying the calculation by taking into account the changes in sample geometry due to thermal expansion and pre-stretching, more exact results were achieved. As one important outcome of this study, an option for taking into account the geometrical error related to the thermal expansion was made in the software provided by the rheometer manufacturer Anton Paar, to be used in conjunction with SER.

A combination of two methods for determining extensional viscosity at broad-extension rate range – considering injection molding simulation as a possible application – was studied in Publication V. Extensional viscosity could be achieved over a wide range of extension rates with relatively good accuracy by measuring it using SER and by evaluating it from contraction flow analysis on capillary rheometry data. Moreover, the molecular stress function (MSF) model could be used to predict the extensional behavior in case where scarce experimental data is available.

Rheological measurements of polymer melts under actual processing conditions, using an adjustable slit die coupled to an injection molding machine, were reported in Publication VI, comparing them to low and moderate shear rate data achieved by conventional off-line rheometers. The viscosity results achieved by the slit die measurements correlated very well with the off-line data, demonstrating the usefulness of a low-cost, easy and fast operation device as a rheological tool. In addition, measurements with three different slit sizes showed a good superposition verifying the absence of wall slip.

PREFACE

This work was carried out between years 2006- 2011 at Tampere University of Technology (TUT), Department of Materials Science. Part of the work, from April 2008 to September 2009, was done during the author's exchange period in Germany at Berlin Institute of Technology (TU Berlin), Chair of Polymer Engineering/ Polymer Physics. The work was inspired by the EU 6th Framework research project "Virtual Injection Moulding for improving production efficiency, quality, and time-to-market speed" (VIM), and carried out under the Graduate School of Processing of Polymers and Polymer-based Multimaterials. They, as well as Academy of Finland, are acknowledged for the financial support.

I gratefully acknowledge Professor Peter Van Puyvelde from K.U. Leuven, Belgium, and PhD Susana Filipe from Borealis Polyolefine GmbH, Austria, for examining this thesis. I express my most sincere gratitude to my supervisor PhD Seppo Syrjälä for always being available for discussion, for tirelessly reviewing my texts, and for teaching me to assess research work objectively and with the necessary criticism. I further acknowledge my custos, Professor Pentti Järvelä for giving me the chance to work at TUT for all these years, and Professor Jyrki Vuorinen for encouraging me in my striving towards the doctoral degree.

I give my special thanks to Professor Manfred H. Wagner for his professional guidance, patience, and true interest towards my work during my stay at Berlin Institute of Technology, and PhD Víctor H. Rolon-Garrído for innumerable fruitful discussions, support and collaboration in preparing manuscripts and conference papers. Further I want to thank the entire staff of the Laboratory of Plastics and Elastomer Technology at TUT as well as the colleagues at Polymer Engineering/ Polymer Physics at TU Berlin for encouragement and help, and for creating a pleasant working environment. I also thank all the partners of VIM consortium for the rewarding cooperation during and even after the project

I sincerely thank all my friends for giving me inspiration, support and the important balance between free time and work. Especially I would like to thank Ms. Tytti Erästö, Dr. Ozgur Dedehayir, Ms. Mari Kylmälä and Ms. Eloise Kok for sharing the ups and downs of research work and doctoral studies. Finally I wish to express my deepest gratitude to all my nearest and dearest: my sisters Helena and Laura, and brothers Tapio, Pirkka, Kalervo and Markus, my dad Markku, and especially my dear Mum Irja, who has supported me all the way and given an outsider's view to my research problems.

Tampere, May 2011

LIST OF ORIGINAL PUBLICATIONS

Peer-reviewed journal publications included in the PhD thesis

I   Aho J, Syrjälä S. On the measurement and modeling of viscosity of polymers at low temperatures. Polymer Testing 27, 2008, 35-40.

II Aho J, Syrjälä S. Evaluation of different methods for determining the entrance pressure drop in capillary rheometry. Applied Rheology 18, 2008, 63258-1 – 63258-5.

III Aho J, Syrjälä S. Measurement of the pressure dependence of viscosity of polymer melts using a back-pressure regulated capillary rheometer. Journal of Applied Polymer Science 117, 2010, 1076-1084.

IV Aho J, Rolón-Garrido VH, Syrjälä S, Wagner MH. Measurement technique and data analysis of extensional viscosity for polymer melts by Sentmanat Extensional Rheometer (SER). Rheologica Acta 49, 2010, 359-370.

V   Aho J, Rolón-Garrido VH, Syrjälä S, Wagner MH. Extensional Viscosity in Uniaxial Extension and Contraction Flow – Comparison of Experimental Methods and Application of the Molecular Stress Function Model. Journal of Non-Newtonian Fluid Mechanics 165, 2010, 212-218.

VI Aho J, Syrjälä S. Shear viscosity measurements of polymer melts using injection molding machine with adjustable slit die. *Accepted for publication:* Polymer Testing, 2011.

AUTHOR'S CONTRIBUTION

For papers I-III the author performed the majority of the experimental work and a share of the writing, excluding the parts involving numerical modeling. In papers IV-V the author performed all the experimental work and the writing excluding the parts involving molecular modeling (MSF theory). In paper VI the author performed all the experiments and majority of writing. All the papers were commented by the coauthors and revised by supervising coauthors Seppo Syrjälä and/ or Manfred H. Wagner.

Other related journal publications and conference papers

Aho J, Syrjälä S. Evaluation of Pressure Dependence of Viscosity for some Polymers Using Capillary Rheometer. 14th Nordic Rheology Conference, June 2005, Tampere, Finland. Annual Transactions of the Nordic Rheology Society 13, 2005, 55-60.

Aho J, Syrjälä S. Determination of the Entrance Pressure Drop in Capillary Rheometry Using Bagley Correction and Zero-length Capillary. 15th Nordic Rheology Conference, June 2006, Stockholm, Sweden. Annual Transactions of the Nordic Rheology Society 14, 2006, 143-137.

Syrjälä S, Aho J. Evaluation of the effect of viscous heating in capillary rheometry of polymer melts. 16th Nordic Rheology Conference, June 2007, Stavanger, Norway. Annual Transactions of the Nordic Rheology Society 15, 2007, 99-103.

Fernández M, Muñoz ME, Santamaria A, Syrjälä S and Aho J. Determining the pressure dependency of the viscosity using pvt data: a practical alternative for thermoplastics. Polymer Testing 28, 2009, 109-113.

Aho J, Rolón-Garrido VH, Syrjälä S, Wagner MH. Extensional viscosity in uniaxial extension and contraction flow – Comparison of experimental methods and application of the molecular stress function model. 18th Nordic Rheology Conference, August 2009, Reykjavik, Iceland. Annual Transactions of the Nordic Rheology Society 17, 2009, 167-173.

Aho J, Rolón-Garrido VH, Syrjälä S, Wagner MH. Study of extensional viscosity in uniaxial extension and contraction flow – Comparison of methods and application of MSF model. Gemeinsame Diskussionstagung der Deutschen Rheologischen Gesellschaft (DRG) und des ProcessNet Fachausschusses "Rheologie", March 2009, Berlin, Germany. Book of Abstracts of DRG, 28.

Aho J, Moog M, Thornagel M, Syrjälä S, Wagner MH. The role of extensional viscosity in injection molding evaluated by contraction flow simulations. Advances in Polymer Science 01, July 2009, Linz, Austria. Proceedings of a Conference on Polyolefins and Polymelamines, 113.

Aho J, Rolón-Garrido VH, Syrjälä S, Wagner MH. Measurement Technique and Data Analysis of Extensional Viscosity for Polymer Melts by Sentmanat Extensional Rheometer (SER). 81st Annual Meeting of the Society of Rheology, October 2009, Madison, WI, USA. Proceedings of the Society of Rheology, 89.

Aho J, Syrjälä S. Pressure dependence of viscosity of polymers and its importance to the simulation of injection molding process" Nordic Polymer Days, May 2010, Helsinki Finland. Book of Abstracts of NPD, 20.

Aho J, Moberg L, Syrjälä S, Järvelä P. Injection molding machine with height-adjustable slit die for rheological measurements of polymer melts under processing conditions. *Accepted for publication*: Annual Transactions of the Nordic Rheology Society, 2011, 19.

LIST OF SYMBOLS AND ABBREVIATIONS

A	material characteristic constant
	surface area
a	fitting parameter in Carreau, Carreau-Yasuda, and Cross equations
a_T, a_p, $a_{T,p}$	horizontal temperature/ pressure/ temperature and pressure shift factor
B	material characteristic constant
b_T	vertical temperature shift factor
C_1, C_2	WLF equation fitting parameters
D	diameter
E	activation energy
F	force
G, g_i	relaxation modulus
G^*	complex modulus
G'	storage modulus
G''	loss modulus
h	gap/ slit height
K	material characteristic constant
L, l	length
L_0	initial length
M_0	torque amplitude
M_w	molecular weight
n	power-law coefficient
n'	local power-law index
N_1	1st normal stress difference
N_2	2nd normal stress difference
p	hydrostatic pressure
Q	volume flow rate
Q_d	drag flow rate
R	ideal gas constant
r, R	radius
R_p	piston radius
T	temperature
t, t'	time

T_g	glass-transition temperature
T_m	melting temperature
T_{ref}	reference temperature
v	velocity
v_1, v_2, v_3	velocity components in directions $x_1, x_2,$ *and* x_3
V_p	piston speed
w	slit width
β	pressure coefficient
γ	strain
γ_0	strain amplitude
$\dot{\gamma}, \dot{\gamma}_0$	shear (strain) rate
$\dot{\gamma}_R$	shear rate at outer rim of the plate-plate rheometer
$\dot{\gamma}_r$	reduced shear rate
$\dot{\gamma}_{wa}$	apparent wall shear rate
$\dot{\gamma}_w$	true wall shear rate
ΔL	differential length
Δp	pressure gradient
Δp_e	entrance pressure drop
δ	phase angle
ε	strain
ε_H	Hencky strain
$\dot{\varepsilon}_H$	Hencky strain rate
η	viscosity
$\eta_0, \eta_{0,np}$	zero-shear viscosity (at normal pressure)
$\eta_{0,p}$	zero-shear viscosity at pressure p
η^*	complex viscosity
η_E	extensional viscosity
η_r	reduced viscosity
η_s	shear viscosity
η'	in-phase component of complex viscosity
η''	out-of-phase component of complex viscosity
η_s^+	start-up shear viscosity
η_E^+	start-up extensional viscosity, uniaxial extension
η_B^+	start-up extensional viscosity, biaxial extension
η_P^+	start-up extensional viscosity, planar extension
λ, λ_i	characteristic (relaxation) time
μ_0	linear viscoelastic limit
ρ	density
ρ_{ref}	reference density
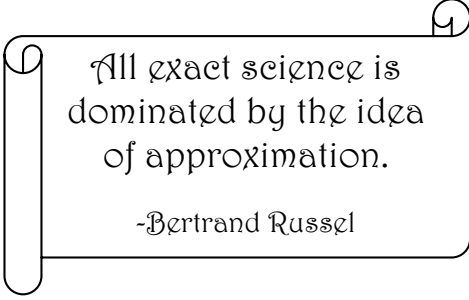
σ_T	tensile stress
τ_{ij}	component ij of $m \times n$ stress tensor
τ, τ_0	shear stress, shear stress amplitude
τ', τ''	in-phase and out-of-phase components of shear stress
τ_c	critical shear stress
τ_e	elastic shear stress
τ_v	viscous shear stress
τ_{wa}	apparent wall shear stress
τ_w	true wall shear stress
Θ_0	cone angle in cone-plate rheometer
φ_0	angular amplitude of oscillatory shear in rotational rheometer initial deflection angle in SER device
Ψ_1	1st normal stress coefficient
Ψ_2	2nd normal stress coefficient
Ω	angular velocity
ω	angular frequency
ABS	acrylonitrile butadiene styrene
CAD	computer aided design
GNF	generalized Newtonian fluid
FEM	finite element method
FSR	filament stretching rheometer
HDPE	high-density polyethylene
LCB	long-chain branch(ing)
LDPE	low-density polyethylene
LVE	linear viscoelastic envelope
MWD	molecular weight distribution
MFR	melt flow rate
MTR	Münstedt tensile rheometer
MVR	melt volume (flow) rate
NPL	National Physics Laboratory
PC	polycarbonate
PMMA	poly methylmethacrylate
PP	polypropylene
PS	polystyrene
pVT	pressure-volume-temperature relation
RME	Rheometrics melt extensiometer
SAOS	small angle oscillatory shear
SER	Sentmanat extensional rheometer
WLF	William-Landels-Ferry equation

TABLE OF CONTENTS

All exact science is
dominated by the idea
of approximation.

-Bertrand Russel

1   INTRODUCTION

Rheology is a study of deformation and flow of matter. Of special interest are the materials which do not follow the Newton's law of viscosity. Newtonian materials flow in the usual way, whereas non-Newtonian materials flow in an unusual way, exhibiting various interesting and peculiar flow phenomena. Rheology therefore is a very interdisciplinary study: Research of non-Newtonian fluids is carried out, for example, in paint and lacquer industry, oil drilling, food industry, pharmacology, and polymer processing. Polymers consist of long chain macromolecules, which largely determine their non-Newtonian flow behavior. They are further defined as viscoelastic materials, which means that their behavior is somewhere between that of elastic solids and viscous fluids.

In order to understand and manage the melt processing of polymers one needs to understand and be able to quantify the rheological phenomena occurring in processing flows. Rheology plays a significant role in determining melt processability of polymers, as well as physical properties of the processed end-products. Despite that, industrial polymer processors often take shortcuts in rheological characterization. This is probably partly due to the tedious nature of experiments or expensive characterization equipment needed, partly because of a belief that some phenomena, such as the ones discussed in this study, do not have a great importance in predicting the flow behavior or interpretation of the results.

 For successful production set up the plastic processors should have a solid understanding of the properties and behavior of the used polymer resins. A consistent data bank including the rheological properties of polymers would benefit the plastic processors who will, using their existing knowledge and the aid of the documented data, tailor the process parameters to suit the properties of each polymer for manufacturing flawless products. Knowledge on rheological behavior of polymers is needed for finding the optimal melt processing conditions, such as temperature and rate of flow, and for estimating the required machine capacity. In addition, rheological data provides essential input for process simulation, which is increasingly adapted as an important part of new process setup and product design. Simulation software is used to enhance the productivity, quality, turnaround times and resource utilization in polymer processing. However, the feasibility of simulation software is strongly dependent on the expertise of the user, the accuracy of the material data and models in its database, and on the understanding of the material behavior. Rheological properties of polymer melts are of particular importance in flow modeling.

Hundreds of different grades of commercial polymers are on the market, and they can have widely varying processing characteristics even within the same base polymer. At present the requirements for manufacturing processes are higher than ever; increasingly finer details and functionalities are implemented in plastic parts, such as combinations of different materials or integration of special functions. At the same time many technical plastic products face very stringent quality requirements such as high strength, small tolerances, dimensional stability, and surface smoothness. Not only the quality of the product, but also the cost effectiveness of the whole process, is

increasingly important. Booming petroleum price raises the polymer raw material costs and, moreover, small- medium size companies in Europe cannot compete in the labor costs with the cheap-labor mass production in emerging industrial countries. In order to keep up with the competition, the consumption of the raw materials and the process cycle time should be kept down and the time and labor needed for the tool design and process setup phases should be minimized. For all the above-mentioned reasons, numerical simulation is achieving an increasingly important role in the part and mould or die design process, as well as in adjusting the right processing parameters for the actual production.

1.1   Scope of the study

In order to increase the competitiveness of European small-medium scale injection molding enterprises, the integrated EU 6th framework project "Virtual Injection Moulding for improving production efficiency, quality, and time-to-market speed" (IP505718-2 VIM) was implemented during 2004-2008. The aim was to increase the efficiency of the molding companies by providing them better tools for optimizing the injection molding process, thus saving time, money and effort related to the optimization of material, mold and process especially at the start-up phase of production. The first task in the project was "Material characterization", which involved measurement of rheological, thermal and mechanical properties of a selected set of commercial polymer grades, in which the author was also involved. These results were utilized to build a data base that was put to use in "Simulation tool development", where the influence of different material parameters on the accuracy of the injection molding filling and packing simulation was studied. This doctoral thesis is partly based on, and inspired by, the studies carried out during the VIM project.

The scope of this study was to add knowledge on the importance of different rheological phenomena in polymer melt processing – especially injection molding – and to improve the rheological measurement techniques. Relevant characterization methods and some difficulties related to them were addressed and examined. The focus was on certain rheological subjects considered important for different polymer processes: pressure dependence of viscosity (Publication III), viscosity of polymers at low temperatures and shear rates (Publication I) and extensional viscosity (Publication V). Experimental procedures for correcting entrance pressure drop in capillary rheometry (Publication II) and extensional viscosity measurements by a uniaxial extension device (Publication IV) were studied and the reliability of the measurements and correct data analysis was discussed. The usefulness of a tailor-made adjustable slit die for rheological measurements using an injection molding machine was demonstrated in Publication VI. The following chapters wrap up the work summarizing the important aspects of polymer melt rheology, rheometry and experimental techniques, and the role of rheology in polymer processing.

2 OVERVIEW TO POLYMER RHEOLOGY

2.1 Basic flow characteristics of polymers

Factors related to the molecular structure of polymers set challenges to their successful processing; unlike metals or ceramics, polymeric materials consist of very long chain-like macromolecules. This leads to rather complex rheological behavior in the molten state. The relationship between elastic shear stress τ_e and strain γ for fully *elastic* materials, such as metals, is determined by Hooke's law.

$$\tau_e = G\gamma \tag{1}$$

For pure *viscous* liquids – such as water, oil, or syrup – deformation is time-dependent, and the relationship between the viscous shear stress τ_v and strain *rate $\dot{\gamma}$* is determined by Newton's law.

$$\tau_v = \eta\dot{\gamma} \tag{2}$$

For *Newtonian* fluids viscosity η is a material constant and not dependent of the rate of deformation. For fully elastic materials the strain is directly proportional to the stress with a factor called shear modulus G (for shear) or Young's modulus E (for tension), and the elastic energy is stored in the substance upon deforming it. Thus the strain is totally recoverable after permitting the material to return to its undeformed equilibrium state, provided that the limit of plastic deformation was not exceeded in loading. For pure viscous materials all the energy is dissipated in the continuous deformation, thus the amount of recoverable strain is zero. The deformation follows the applied stress with delay[1].

The properties of polymer melts lie somewhere between Hookean and Newtonian materials, thus they are *viscoelastic* liquids by nature. Cross-linked rubbers have properties closer to the elastic materials and they are often referred to as viscoelastic solids. Viscoelasticity makes the materials' response to stress-strain behavior time dependent and their deformation partially reversible. Polymer melts are further defined as *non-Newtonian* fluids: their viscosity is not constant, thus the relationship between deformation rate and stress is not linear. The reasons for non-Newtonian behavior can be found in the molecular structure: Polymers consist of long molecules that entangle with each other, forming several flexible, reversible "joints". These enable different conformations of the molecules by a rotation along the backbone and cause the elastic behavior of polymer melts. The chains can also move with respect to each other by a crawling kind of movement called reptation. These rotation and reptation occurring above the glass transition temperature of the polymer are called Brownian motions, and they tend to return the molecules towards the equilibrium, i.e., to the energetically most preferable state, after being oriented by applying deforming stress. This will not,

however, occur immediately after removing the stress but within a certain relaxation time, dependent on the molecular characteristics of the polymer[1].

From the polymer processing point of view, among all non-Newtonian phenomena the most important one for polymer melts is their common *shear thinning* characteristic, which means that their viscosity decreases as a function of shear rate. This occurs due to orientation and disentanglement of the entangled macromolecules in the melt when a certain critical shear rate (limit of the linear viscoelasticity; change from the zero-shear viscosity to shear thinning behavior) is exceeded. Shear thinning is actually the property that ultimately enables many of the melt processing techniques of polymers[1].

2.1.1 Linear viscoelasticity and mechanical models

When very small deformation is applied to the polymer melt, or when the deformation rate is very slow, the molecules have enough time to relax through the Brownian motion and the polymer structure remains unaltered; the entangled and coiled state of the molecules is not disturbed. The deformation is said to be in the *linear viscoelastic range.* For characterizing the inherent material properties in rheological experiments, it is essential that the measurements are done in the linear viscoelastic range, i.e. the deformation is kept small enough. The relaxation of the molecules is described by relaxation modulus G. According to the Boltzmann superposition principle, in the linear viscoelastic region the response of a material to series of step strains is a sum of the responses of the each step (total stress $\tau(t)$ is the sum of stresses generated at each step from time t' to t. $\dot{\gamma}$ is the shear rate):

$$\tau(t) = \int_{-\infty}^{t} G(t - t')\dot{\gamma}(t')dt' \tag{3}$$

The responses of viscoelastic materials to applied stress or strain can be modeled with the aid of mechanical spring-dashpot analogies. The dashpot describes the viscous, and the spring the elastic response to the applied load or deformation. The dashpot represents the time dependence and relates to the characteristic relaxation time of a material, the time the molecule needs to return to the equilibrium state after deformation[1].

The Maxwell model consists of a dashpot and spring in series (Figure 1a) and is a simplest model to describe the behavior of viscoelastic liquids. As can be figured from this setting, the dashpot allows for indefinite deformation; for a viscoelastic fluid no limiting cross-links exist, unlike in viscoelastic solids. The Maxwell model describes the stress relaxation of a polymer: decay of the stress at a constant, pre-defined strain. However, the one-element Maxwell model alone is not able to describe the stress relaxation behavior of true viscoelastic liquids, as they are always more complex systems consisting of distribution of molecule chains lengths. The generalized Maxwell model (Figure 1b) consists of series of *n* Maxwell elements, and gives a closer-to-reality picture of the behavior of viscoelastic fluids, such as polymer melts above their glass transition and melting temperatures. It describes the relaxation time spectrum of a polymer; each length of molecule has a characteristic relaxation time and each element represents one of them.

The Kelvin model (also called the Kelvin-Voigt or Voigt model) combines one dashpot and one spring in parallel (Figure 1c), modeling the behavior of viscoelastic solids, such as cross-linked rubbers. This model describes the *creep* and *creep recovery* behavior; constant loading condition causes a "creeping" – time dependent strain deformation – of the material. Similarly, the strain recovery after stress removal does not occur instantaneously but depends on the material's characteristic time. The Kelvin model allows for a completely recoverable strain, thus it does not describe the creep

recovery behavior of molten thermoplastics correctly. For modeling the creep of polymer melts, at least one dashpot element has to be added in series with the Kelvin model in order to model the non-recoverable portion of strain. In a creep test a constant stress is applied to the sample, and the following deformation strain is recorded. When the applied stress is removed, strain recovery is observed: The material returns partially to the original, undeformed state[2,3].
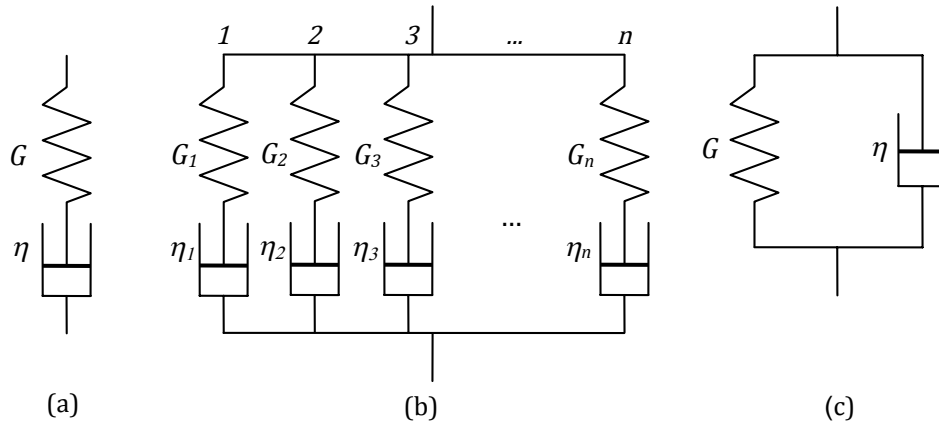

Figure 1. Representation of the Maxwell model (a), the generalized Maxwell model (b), and the Kelvin model (c)

The behavior of real polymer systems in creep or stress relaxation can be modeled using the different combinations of mechanical model analogies presented above, nevertheless, they do not describe the structure of viscoelastic solids or liquids physically, neither give quantitative information of viscoelasticity. Creep/creep recovery, stress relaxation, and *small amplitude oscillatory shear* (SAOS) experiments are used to characterize the linear viscoelastic properties of polymers. SAOS involves dynamic load of the material at small pre-defined strain amplitude at changing frequency. In oscillatory shear the deformation is sinusoidal – provided that the deformation is in the linear viscoelastic region – and the viscoelasticity manifests itself as a phase lag between the applied stress and the strain (Figure 2). The phase lag between stress and strain is expressed as the phase angle δ.
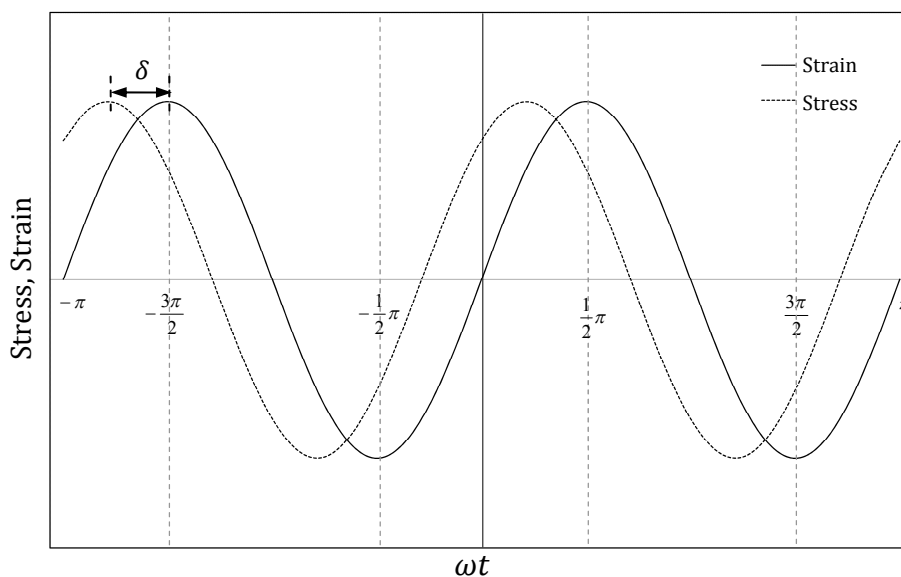

Figure 2. Sinusoidal forms of stress and strain for a viscoelastic substance.

The strain function has the form

$$\gamma = \gamma_0 \sin \omega t \tag{4}$$

γ_0 = strain amplitude and ω = angular frequency. Correspondingly, the stress is

$$\tau = \tau_0 \sin(\omega t + \delta) \tag{5}$$

Stress consists of in-phase (τ') and out-of-phase (τ'') components, from which the first one relates to the elastic and the latter one to the viscous part of the response to applied strain:

$$\tau = \tau' + \tau'' = \tau_0' \sin \omega t + \tau_0'' \cos \omega t \tag{6}$$

The out-of-phase component of the stress is in phase with the strain rate, which is the time derivative of the small-amplitude strain:

$$\dot{\gamma} = \frac{d\gamma}{dt} = \dot{\gamma}_0 \cos \omega t \tag{7}$$

where $\dot{\gamma}_0$ = strain rate amplitude. The viscoelastic moduli: *storage modulus G'* representing the elastic part i.e. the amount of energy stored in the material and the *loss modulus G"* representing the viscous part, i.e. the energy dissipated in the deformation are:

$$G' = \frac{\tau_0'}{\gamma_0} \qquad G'' = \frac{\tau_0''}{\gamma_0} \tag{8}$$

The relation between the viscoelastic moduli is called the loss factor:

$$\tan \delta = \frac{G''}{G'} \tag{9}$$

The relation between the moduli and frequency can be expressed as magnitude of *complex viscosity* (from this point onwards simply 'complex viscosity') consisting of the viscous and elastic parts:

$$|\eta^*| = \sqrt{(\eta'^2 + \eta''^2)} = \sqrt{\left[\left(\frac{G'}{\omega}\right)^2 + \left(\frac{G''}{\omega}\right)^2\right]} = \frac{|G^*|}{\omega} \tag{10}$$
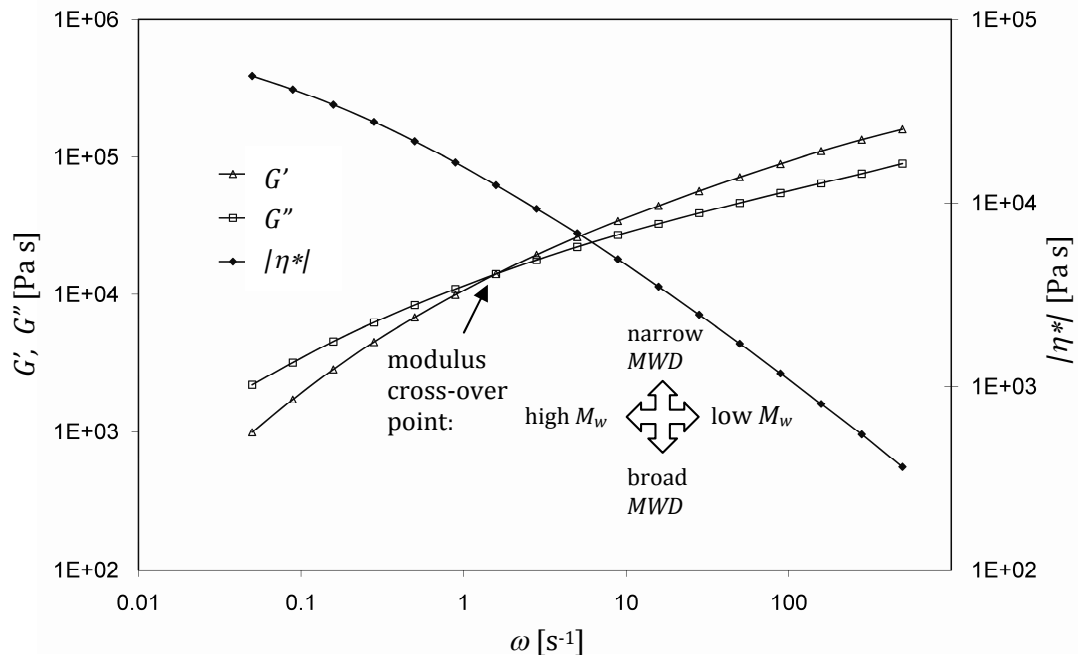
Figure 3. Result curves from a typical SAOS test. Location of the cross-over point of _G′_ and _G″_ gives information about the molecular weight and molecular weight distribution.

In SAOS tests the dynamic moduli vs. frequency are determined from the stress vs. strain response of the material. At low frequencies the loss modulus is higher, thus the material behaves more like a liquid, while at high frequencies the storage modulus, and thus the solid-like behavior, dominates. The cross-over point of the curves, where $G'=G''$, gives an indication of the average molecular weight (M_w) and breadth of the molecular weight distribution (MWD) of polymers as shown in Figure 3. _Long-chain branching_ (LCB), which is present for example in the molecular structure of low-density polyethylene, increases the elasticity of the melt and shifts the modulus cross-over point to the left[2].

2.1.2 Non-linear viscoelasticity

When the deformation amplitude or rate is increased, the entanglements of molecule chains start to reorganize and orientate along the flow. This means that the deformation exceeds the limit of linear viscoelasticity and the melt structure is destroyed. The material response becomes dependent on the rate, kinematics and magnitude of deformation, and the load is said to be in the _non-linear_ region. In the polymer melt processing the extent of deformation is not small and slow but occurs in the non-linear region, and in order to get information about the melt behavior in processing flows, rheological measurements in the non-linear viscoelastic region are important.

Description of the material response in the non-linear world gets more complex because of the need to include deformation and deformation rate into consideration. In other words, a property, such as shear viscosity, is always dependent on the shear rate, and those measured at different strain rates are not comparable to each other. Moreover, one has to consider the deformation kinematics; thus the extensional behavior of a material cannot be derived from shear experiments or vice versa. The real-world phenomena, such as those occurring in plastics processing, most often involve rapid and large deformations, thus the need for knowledge of non-linear behavior is clear.

Newtonian fluid flow exhibits only a stress component in the flow direction (x_1, see Figure 4 on page 11), whereas in polymer melts also normal stresses, that is, stress components in the parallel directions (Figure 4, x_2 and x_3), are found due to the fluids' viscoelastic nature. As polymer melts in normal cases are considered incompressible, the normal stresses are isotropic, and do not cause any deformation. Therefore the absolute normal stress values have no rheological significance. However, the difference between the normal stresses acting in different directions causes deformation and is significant from the rheological point of view. For simple shear flow normal stresses are thus expressed as normal stress differences: the difference between the 1st and 2nd diagonal component (1st normal stress difference N_1) and the difference between the 2nd and 3rd diagonal component (2nd normal stress difference N_2) in the tensor notation for the shear stress[1].

At the steady-state of a start-up flow or creep flow the non-linear rheological behavior of the polymer can be fully described with the aid of three viscometric functions that depend on shear rate; viscosity η, 1st normal stress coefficient ψ_1 and 2nd normal stress coefficient ψ_2:

$$\eta(\dot{\gamma}) = \frac{\tau_{21}}{\dot{\gamma}_0} \tag{11}$$

$$\psi_1(\dot{\gamma}) = \frac{\tau_{11} - \tau_{22}}{\dot{\gamma}_0^2} \tag{12}$$

$$\psi_2(\dot{\gamma}) = \frac{\tau_{22} - \tau_{33}}{\dot{\gamma}_0^2} \tag{13}$$

where τ_{11}, τ_{22}, and τ_{33} are the diagonal components of the stress tensor. $\psi_1(\dot{\gamma})$ is usually regarded as positive-signed, whereas $\psi_2(\dot{\gamma})$ has an opposite sign and its magnitude is only a fraction of that for $\psi_1(\dot{\gamma})$. Most commonly in determining the polymer properties for processing purposes, the quantity of major interest is the shear viscosity as a function of shear rate. In fact, the determination of normal stress differences is much more complicated than that of $\eta(\dot{\gamma})$, and lot less is known about them. However, the normal stress coefficients give important information about the viscoelastic properties of the melt and are, together with other rheological measures, significant in characterizing molecular structures: η_0 and $\psi_1(\dot{\gamma})$ are both proportional to the molecular weight of the polymer[1,2,3]. Moreover, observing changes in normal stress differences during the step-strain measurements by cone-plate and plate-plate experiments gives indications about edge flow instabilities[4], and has also been related to the instabilities occurring in extruding flows, for example in capillary rheometry[5].

2.1.3 Cox-Merz rule

An empirical rule found out by Cox and Merz[6] creates a link between the linear and non-linear quantities. If the Cox-Merz rule is applicable, the complex viscosity from SAOS test and steady-shear viscosity can be combined so that

$$\eta(\dot{\gamma}) = |\eta^*(\omega)|, \text{ when } \dot{\gamma} = \omega \tag{14}$$

Originally, the rule was found to hold for two different polystyrenes between dynamic data and capillary rheometry data. In capillary rheometry, issues such as entrance pressure drop and pressure effects can impair the compatibility of data, thus the applicability of the rule depends on the polymer in question and must in unclear cases be separately checked. The two before-mentioned factors naturally do not affect the

compatibility if dynamic data is combined with steady-shear data from a rotational rheometer.

The advantage of applying the Cox-Merz rule is the smaller number of experiments needed for characterization: both linear viscoelastic characteristics and non-linear flow properties can be extracted from same measurements. Moreover, the maximum shear rate range of the rotational rheometer is 'extended': in the steady step-shear mode the maximum rate due to arising edge fracture (see Chapter 3.1) is about 10 s^{-1}, but in the dynamic mode rheometers can typically be operated at up to 100 Hz, which corresponds to an angular frequency of 628 s^{-1}.

2.1.4   Temperature dependence and time-temperature superposition

Polymer molecules constantly exhibit a so called Brownian motion; they can move past each other, rotate and reptate in large number of possible conformations due to their length and flexibility. The Brownian motion of an individual chain is largely inhibited by the other molecules surrounding it. This is also referred to as entanglements of the chains, although the chains do not necessarily need to be looped together; the chains packed closely together in the melt just do not have space, thus they are inhibiting each others' motions[2]. When the temperature of the melt is increased, the Brownian motions of the chains augment and the *free volume* around the polymer chains increases. Increased free volume means easier flow, and decreased viscosity[7].

The extent to which the viscoelastic properties are dependent on temperature is traced back to the molecular structure of the polymer chains: The more complex the structure – i.e. the more branches, large pendant groups, and ring structures it has – the stronger the effect of temperature on the viscosity, since the greater is then the relative change in the free volume as a function of temperature[7]. In order to make the polymer melt to flow, the chain segments must have enough free space around them and there must be enough thermal energy to overcome the motion-inhibiting barriers, such as rotation around covalent bonds[1].

If the viscoelastic functions of a polymer measured at different temperatures can be shifted by a single shift factor to one, selected reference temperature to form a *master curve* with a good superposition, the material is *thermo-rheologically simple*, meaning that all the relaxation times have the same temperature dependence. Quantities including a stress component, such as the storage and loss moduli, are shifted by multiplying with a *vertical shift factor* b_T and the quantities including time, such as frequency or shear rate, with *horizontal shift factor* a_T. This procedure is called the *time-temperature superposition* (TTS). If TTS is valid and shift factors can be used to create a master curve from linear viscoelastic data, the same shift factors should in principle be also applicable for shifting non-linear data, e.g. viscosity as a function of shear rate. When the quantity to be shifted includes both time and stress, like viscosity does, both horizontal and vertical shift factors should be applied: the viscosity is shifted by multiplying with the factor b_T/a_T to yield the 'reduced' viscosity η_r

$$\eta_r = \frac{\eta(\dot{\gamma},T)b_T}{a_T} \tag{15}$$

and the reduced shear rate is obtained by shifting $\dot{\gamma}$ with a_T

$$\dot{\gamma}_r = a_T\dot{\gamma} \tag{16}$$

The vertical shift factor is given as

$$b_T = \frac{T_{ref}\rho_{ref}}{T\rho} \tag{17}$$

with T = temperature and ρ = density, and T_{ref} and ρ_{ref}, respectively are the reference temperature and pressure. However, the vertical shift factor b_T is relatively insensitive to temperature, and often taken to be unity. Then the viscosity can be shifted by the horizontal shift factor only, and has the form

$$\eta_r = \frac{\eta(\dot{\gamma},T)}{a_T} \tag{18}$$

The horizontal temperature shift factor at $T \leq T_g + 100$ K can be described according to Williams, Landel and Ferry (the WLF equation)[8] as

$$\log a_T = -\frac{C_1(T-T_{ref})}{C_2+(T-T_{ref})} \tag{19}$$

with C_1 and C_2 as fitting parameters. When $T_{ref} = T_g$ these parameters have been observed to have universal constant values C_1 = 17.44 and C_2 = 51.6 K, based on a fitting on a large number of polymers. The more accurate approximation with WLF equation was found when T_{ref} was not treated as a fixed parameter but allowed to be adjusted being ~50 K above the glass transition temperature. This was accomplished with the constants C_1 = 8.86 and C_2 = 101.6 K[8]. At temperatures higher than T_g + 100 K the free volume is no longer a limiting factor, but the energy barriers resisting the flow become significant. Then the temperature dependence is better expressed by the Arrhenius equation[7]:

$$a_T = exp\left[\frac{E}{R}\left(\frac{1}{T}-\frac{1}{T_{ref}}\right)\right] \tag{20}$$

where E is the activation energy of flow and R = ideal gas constant = 8.314 J/mol·K. The activation energy of flow gives an indication about the molecular structure and chain branching[9]: typically polymers with LCB structures have higher E than the linear ones.

The master curve presentation is sometimes used even when a material shows thermo-rheological complexity. In such cases no information about the molecular features of the polymer can be achieved from the master curves, however, they show the general trend of rheological behavior over a wide range of deformation[10].

2.1.5   Pressure dependence

Generally fluids, such as polymer melts, are considered incompressible. Nevertheless, at high hydrostatic pressures that can occur in melt processing, they do exhibit some compressibility. Therefore pressure also has an effect on viscosity, albeit not nearly as strong as temperature. The pressure dependence of viscosity of polymer melts has a practical significance in high-pressure processes, such as injection molding, where pressure frequently exceeds 100 MPa. In an analogous manner to the temperature dependence, viscosity as a function of pressure obeys exponential behavior, but with an inverse effect: the free volume between the molecules decreases when the pressure increases, and thus the Brownian motions of the chains are more inhibited. Therefore an increase in pressure also increases viscosity. A common way to describe the pressure effect on viscosity is to use the Barus equation

$$\eta_{0,p} = \eta_{0,np}e^{\beta p} \tag{21}$$

where and $\eta_{0,np}$ = zero-shear viscosity at normal (atmospheric) pressure, p = pressure and β = material-characteristic pressure coefficient. The pressure shift factor is thus

$$a_p = e^{\beta p} \tag{22}$$

In the vicinity of the T_g the effect of pressure, as also the effect of temperature, is larger than at higher temperatures[11]. Pressure induced crystallization can also occur at elevated pressures, causing solidification above the T_m of atmospheric pressure, and this naturally causes a strong increase in melt viscosity[1].

According to Cogswell[12] the pressure dependence can be expressed in terms of equivalent change in temperature as a pressure-temperature coefficient $(dT/dp)_\eta$ which has an average value of -5 x 10^{-7} K/Pa meaning that an increase of pressure by 100 MPa would correspond to a decrease of temperature by 50 K. The exact value of the coefficient varies depending on the polymer in question in the same way as for the temperature dependence.

2.2 Viscometric Flows

Two types of flows are commonly studied for non-Newtonian fluids: *simple shear* and *simple elongational (extensional) flow*. Shear flow takes place in various industrial processes, and is also the easiest flow type to generate in laboratory circumstances. Simple shear is uniform flow: each fluid element on a same stream line undergoes exactly the same deformation and the distance between them remains unchanged (Figure 4).
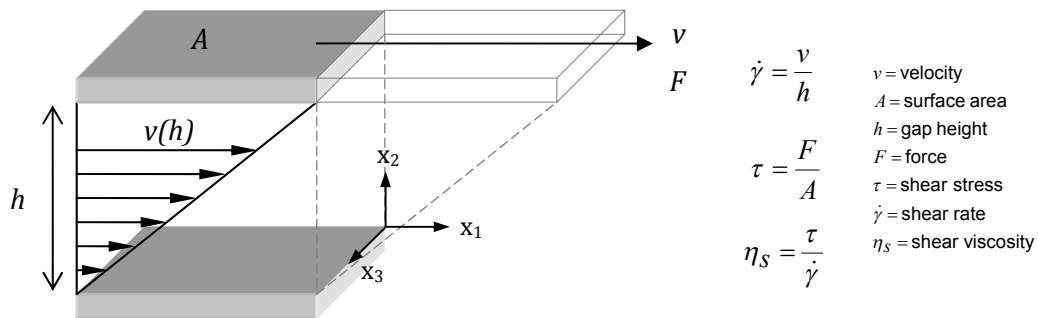

Figure 4. Representation of velocity fields in simple shear flow

The term *viscometric flow* embodies both the uniform, simple shear flow and the non-uniform shear flows that occur in rheometry and common processes, and where the fluid behavior can be governed by three functions; viscosity, first and second normal stress coefficients. Viscometric flows can be divided into *drag flow* and *pressure driven flow* (*Poiseulle flow)* according to the way the shear is created: in drag flow shearing is generated between two surfaces, moving the one while keeping the other stationary, as for simple shear in Figure 4. In pressure-driven flow, shearing occurs due to the pressure gradient in a closed channel. *Tube* or *capillary flow* is the pressure-driven flow most commonly used to measure the shear viscosity of polymers. This type of flow occurs in circular channels and slits and can be described as a telescope-like behavior of fluid elements, where the velocity at the centerline of the flow is at highest and zero next to the wall, assuming that no slip occurs between the wall and the melt (Figure 5). Correspondingly the shear rate is at highest on the wall, and zero on the centerline[1,3].
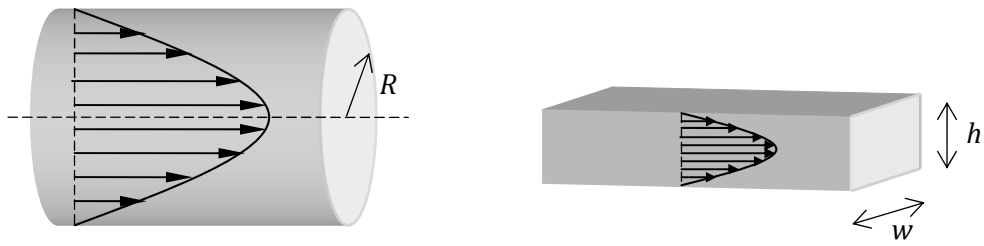
Figure 5. Representation of velocity fields in pressure-driven tube and slit flow.

2.3 Extensional Flows

Besides shear flow, melt can experience extensional (or elongational) flow during processing. This means that the material undergoes stretching along the streamlines as a consequence of extensional deformation and the distance between particles on the same streamline changes. The simplest extensional flow type is *uniaxial extension:* stretching of the material in one direction causes compression in the other two directions. In *biaxial extension* the velocity profile is the same as for uniaxial flow, but the extension rate is always negative (compression), whereas for uniaxial flow it is always positive (tension). In *planar extension* one dimension of the material is extended while the second one is maintained constant and the third one compressed (Figure 6)[1,2].

uniaxial

$$v_1 = \dot{\varepsilon}(t)x_1$$
$$v_2 = -\tfrac{1}{2}\dot{\varepsilon}(t)x_2$$
$$v_3 = -\tfrac{1}{2}\dot{\varepsilon}(t)x_3$$

biaxial

$$v_1 = \tfrac{1}{2}\dot{\varepsilon}(t)x_1$$
$$v_2 = \tfrac{1}{2}\dot{\varepsilon}(t)x_2$$
$$v_3 = -\dot{\varepsilon}(t)x_3$$

planar

$$v_1 = \dot{\varepsilon}(t)x_1$$
$$v_2 = 0$$
$$v_3 = -\dot{\varepsilon}(t)x_3$$
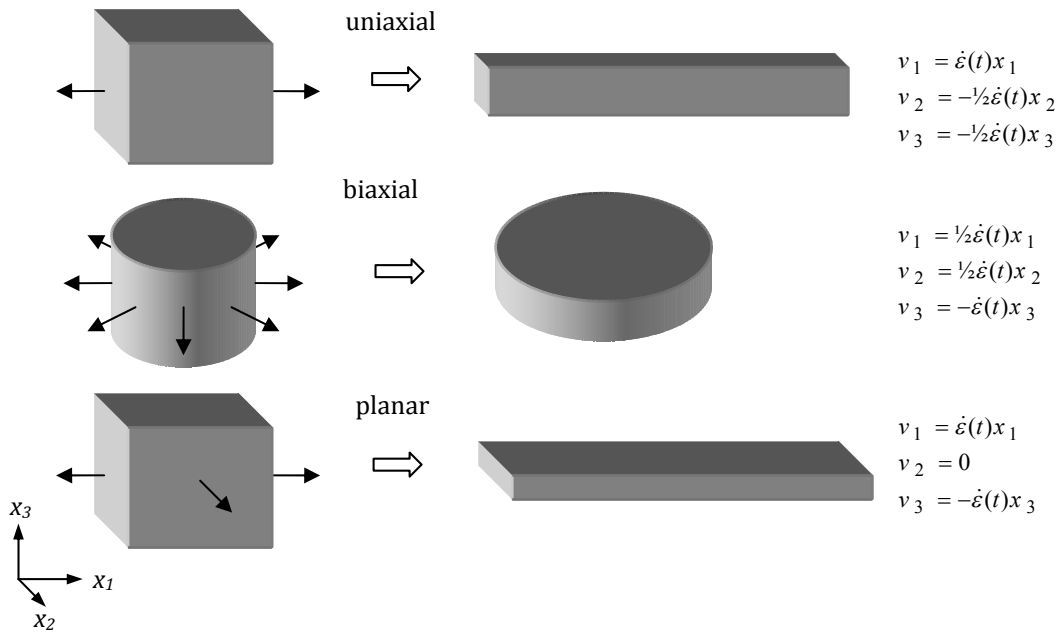
Figure 6. Uniaxial, planar, and biaxial extension and their velocity distributions

Typical curves of start-up test in uniaxial extension are given in Figure 7. Trouton's rule links shear and extensional properties together: in the linear region the curve should obey the *linear viscoelastic envelope* (LVE), which in uniaxial extension is three times the start-up shear viscosity η_s^+ when the shear rate is within the Newtonian flow region and viscosity thus independent of shear rate (Equation 23). In biaxial extension the multiplication factor is 6 (Equation 24), and in the planar case 4 in the x_1 direction and 2 in the x_2 direction (Equation 25).

$$\lim_{\dot{\varepsilon}_H \to 0} |\eta_E^+(t, \dot{\varepsilon}_H)| = 3\eta_s^+(t, \dot{\gamma} \to 0) \tag{23}$$

$$\lim_{\dot{\varepsilon}_H \to 0} |\eta_B^+(t, \dot{\varepsilon}_H)| = 6\eta_s^+(t, \dot{\gamma} \to 0) \tag{24}$$

$$\lim_{\dot{\varepsilon}_H \to 0} |\eta_{P1}^+(t, \dot{\varepsilon}_H)| = 4\eta_s^+(t, \dot{\gamma} \to 0)$$
$$\lim_{\dot{\varepsilon}_H \to 0} |\eta_{P2}^+(t, \dot{\varepsilon}_H)| = 2\eta_s^+(t, \dot{\gamma} \to 0) \tag{25}$$

Parameter $\dot{\varepsilon}_H$ is the Hencky strain rate (logarithmic strain rate), which provides a correct measure of the strain rate when the deformation takes place in increments.
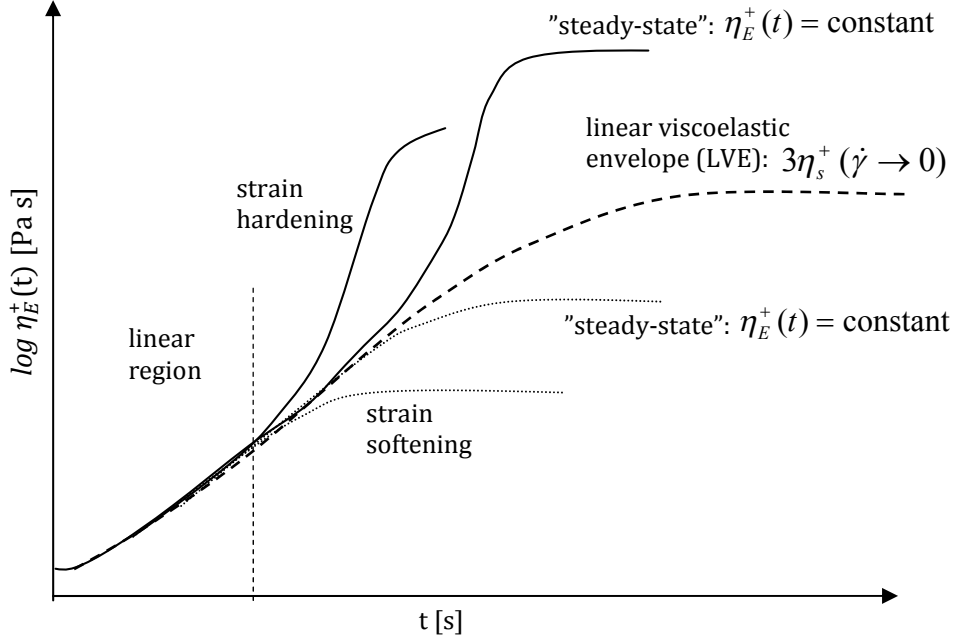

Figure 7. Start-up uniaxial extensional flow of polymer melts. Strain hardening behaviour is illustrated by solid lines and strain softening behaviour by dotted lines.

Non-linearity manifests itself as a deviation from the LVE: for *strain-hardening* materials the curves start to rise steeply before levelling off to a *steady-state*, where the viscosity becomes independent of time. For *strain-softening* materials the non-linearity appears as a steady-state level below the LVE. The steady-state flow may be difficult to observe in experiments, as instability of the sample and limitations of the test device often impair this.

Strong strain hardening in extensional flow is common for LCB polymers, and is attributed to the branched structure that efficiently constrains the flow: the steep rise in the start-up curve can be postulated to be caused by the stretching of the backbone between the branch points. Strain hardening can also be observed in linear polymers that have a bimodal MWD with small amount of very high-M_w fractions[2].

In most industrial melt processes the flow is a mixture of both elongational and shear flows: there is almost always stretching along the streamlines at some stage of the process. For example in injection molding, elongational flow occurs at gates and sudden changes in flow cross section where the melt accelerates, as well as at the front of the fountain-flow pattern in the cavity. Shearing is, however, a dominant deformation type in the mould cavity where the melt flows along the mold wall. Elongational flows dominate, for example, in film blowing, blow molding and fiber spinning processes, and in engineering of polymer resins for those applications the determination of extensional properties is crucial[1,13]. Most often the extensional characterization is done in uniaxial extension, which most conveniently and effectively reveals strain hardening important

for processing methods involving extensional flow. Planar flow seems to mirror the uniaxial extension regarding the strain-hardening function, and biaxial flow behavior is closest to shear flow with only minor strain hardening[13].

When the steady-state extensional viscosity values from start-up flow are plotted against Hencky strain rates, polymers with strong strain hardening in start-up flow typically exhibit a constant $\eta_E(\dot{\varepsilon}_H)$, then *extension thickening* at increasing $\dot{\varepsilon}_H$, followed by an *extension thinning* region in a similar manner to shear flow (Figure 8). However, not all strain hardening polymers necessarily have the extension thickening behavior over the same range of strain rates[2].
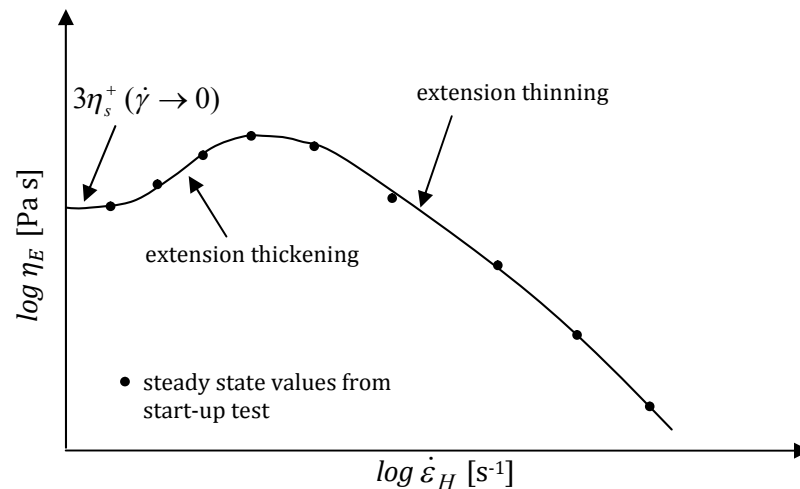
Figure 8. Typical curve of extensional viscosity vs. Hencky strain rate for an extension-thickening polymer

2.4   Viscosity models for shear-thinning polymer melts

Different models are used to describe the flow behavior of shear-thinning fluids. By fitting a model to the experimental data set, the flow behavior over wider than experimental range of shear rates can be predicted. The amount of free model parameters, as well as the models' predicting capability varies, some being more suitable e.g. for broad MWD polymers (gradual transition from Newtonian plateau to shear-thinning region) and some for narrow MWD polymers (sharp transition between Newtonian and shear-thinning regions). A typical shear viscosity curve for a polymer melt with different flow regions is presented in Figure 9, along with the parameters contributing to the fitting at each region.

Figure 9. Typical shear viscosity curve for shear-thinning polymer melt

Power-Law –model (also: Ostwald – de Waele model) is the simplest viscosity model requiring two fitting parameters: K and n:

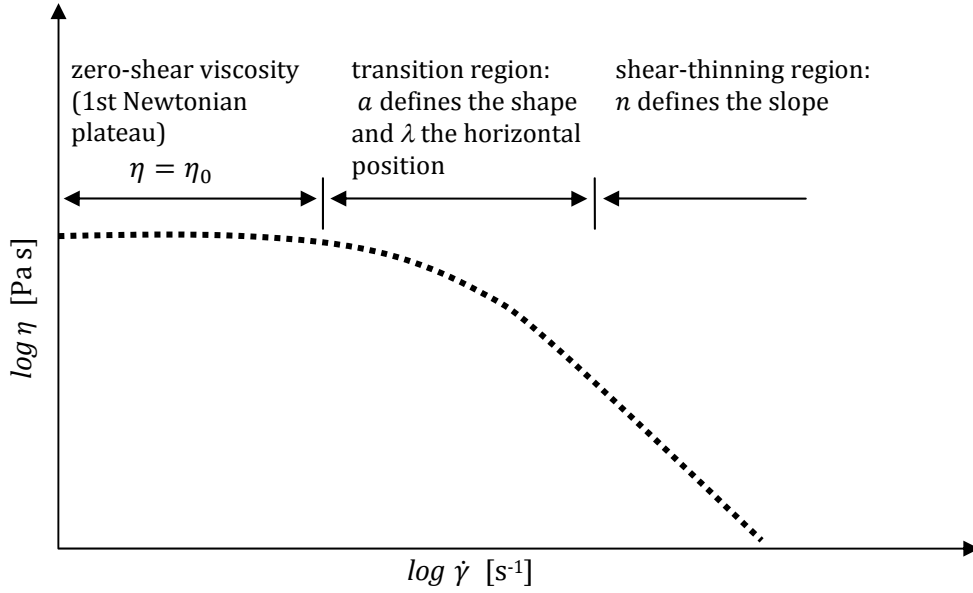$$\eta(\dot{\gamma}) = K\dot{\gamma}^{n-1} \tag{26}$$

$n-1$ is the slope of $\log\eta$ vs. $\log\dot{\gamma}$, thus for Newtonian materials n = 1, for shear-thinning material n < 1, and for shear-thickening materials n > 1. K relates to the magnitude of the viscosity being the vertical axis intercept on the *log* viscosity vs. *log* shear rate plot. The model is capable of describing either only Newtonian flow, or shear thinning (or shear thickening), and is thus of less use for polymer melts that show a Newtonian plateau at low shear rates and shear thinning at high shear rates. The Cross model is capable of describing Newtonian viscosity, shear-thinning viscosity, and also the transition area between them

$$\eta(\dot{\gamma}) = \frac{\eta_0}{1+(\lambda\dot{\gamma})^{1-n}} \tag{27}$$

with fitting parameters: η_0= zero-shear viscosity, n= power-law coefficient, and λ= characteristic time. For certain polymers a better fit at the transition area is achieved by the Carreau model

$$\eta(\dot{\gamma}) = \eta_0 \left[1 + (\lambda\dot{\gamma})^2\right]^{\frac{n-1}{2}} \tag{28}$$

Factor 2 in the exponents of the model makes the shift from zero-shear viscosity to Power-law area sharper. This model therefore describes best the viscosity function of narrow MWD polymers. The Carreau-Yasuda model has one freely adjustable parameter – a – more than the Cross and Carreau models, thus it is able to describe more gradual transition from Newtonian plateau to the shear-thinning region,

$$\eta(\dot{\gamma}) = \eta_0 \left[1 + (\lambda\dot{\gamma})^a\right]^{\frac{n-1}{a}} \tag{29}$$

therefore allowing a good fit also for polymers with broader MWD (long chain branched polymers). The Cross and Carreau models are actually only variations of the Carreau-Yasuda model, both having a fixed parameter for the curvature of the transient region

from Newtonian to shear-thinning behavior. For Cross model $a = 1 - n$, making the curvature dependent on the shear-thinning of viscosity, and for Carreau model $a = 2$. The latter offers the least flexibility of these three models, and the fitting suits well only for polymers with sharp transition area, i.e. for polymers with relatively narrow MWD[3,14].

Temperature and pressure effects can be included in the fitting using a coefficient based either on the Arrhenius or WLF equation for temperature, and the Barus equation for pressure. Acknowledging both the temperature and pressure effect in the viscosity fitting is done by multiplying the individual shift factors a_T and a_p and including the total shift factor in the viscosity model, as for example here in the Carreau-Yasuda fitting:

$$\eta(\dot{\gamma}) = a_{T,p}\eta_0 \left[1 + (a_{T,p}\lambda\dot{\gamma})^a\right]^{\frac{n-1}{a}} \tag{30}$$

The viscosity models presented here are extensions of Newtonian constitutive equation (Equation 2) for viscous fluid flow. Unlike the Newtonian equation, they can also model the shear rate dependence of viscosity and are therefore called constitutive equations for *generalized Newtonian fluids* (GNF). Viscoelasticity, and thus for example the normal stress differences, cannot be described by GNF models[3].

3   RHEOMETRY AND GOOD MEASUREMENT PRACTICE

Devices for shear rheology measurements can be roughly divided into drag-flow and pressure-flow based. Extensional properties can be measured using devices operating either in uniaxial, planar, or biaxial extension. Several types of devices for both shear and extensional flow exist, and only the ones used within this study are introduced in the following sections.

3.1   Cone-plate and parallel-plate rheometry

Drag flow can be generated, for example, by parallel-plate (plate-plate) or cone-plate geometries connected with rotational rheometers, which are commonly used for measuring the viscometric and viscoelastic functions of polymer melts. Drag flow between two rotating or oscillating plates is often called torsion flow due to the kinematics of the system. In the strain-rate controlled mode the deformation rate is set and the resulting torque recorded, and in the stress-controlled mode the torque is a pre-set value and the deformation is the measured quantity. Many rheometers are able to operate in both modes whereas some are limited to either stress or strain control. Only a very small sample amount is needed, and the tests can be run in either step-strain mode (shear rate profile from low to high rates or vice versa) or oscillatory (dynamic) mode. Rotational rheometers typically have very accurate temperature control in isothermal tests (convection oven used at $T > 200$ °C) and high torque resolution. The limitation of the function is usually set by the maximum deformation rates and stresses: flow instabilities, such as edge fracture (breakage of the sample layer between the plates) start to occur when the stress and strain become too high. Often the maximum shear rate in strain-rate controlled rheometers is less than 10 s^{-1}, but it varies by polymer depending also on the viscoelasticity of the sample[5], and the gap at the rim (thus in case of cone-plate configuration, on the cone angle)[15]. The maximum measurable torque is commonly ~200 mNm which limits experimentation on high-viscous materials such as cross-linking rubbers or any polymer melt at very low temperature. The parallel-plate and cone-plate geometries are illustrated in Figure 10.
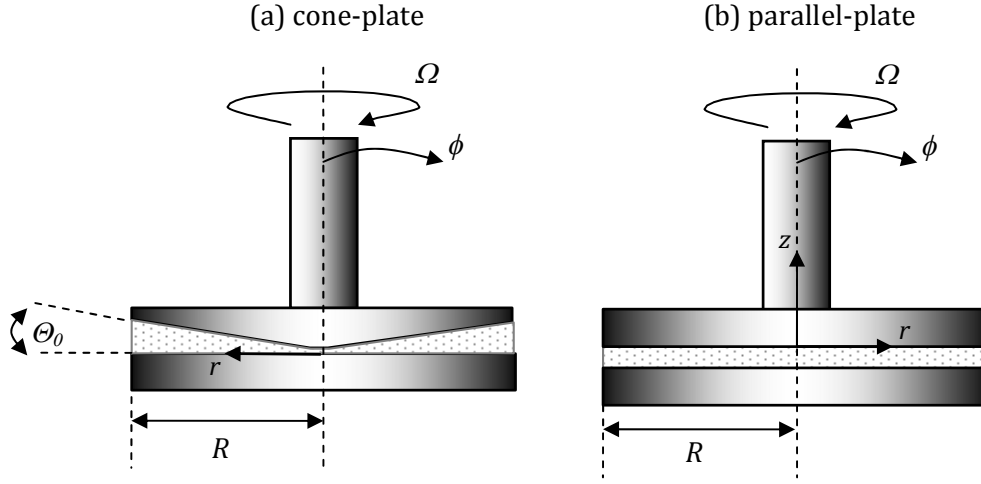
Figure 10. Principle of cone-plate and parallel-plate rheometer geometries

The cone-plate rheometer is the most popular device for measuring non-linear properties at small deformation rates. The upper part of the geometry has a conical profile with a truncated tip, which produces the uniform shear rate profile throughout the gap (Figure 10a). The gap between the cone and plate in the measurement position is determined by the imaginary tip of the cone, which would touch the lower plate. The shear rate is determined by angular velocity Ω and the angle between the cone and the plate Θ_0

$$\dot{\gamma} = \frac{\Omega}{\Theta_0} \tag{31}$$

The shear stress is

$$\tau = \frac{3M}{2\pi R^3} \tag{32}$$

and the shear viscosity thus

$$\eta = \frac{3M\Theta_0}{2\Omega\pi R^3} \tag{33}$$

The cone-plate system can also be used in dynamic (oscillatory) mode to measure linear viscoelastic properties. Then the SAOS functions are calculated as follows:

$$G'' = \frac{3\Theta_0 M_0 \sin\delta}{2\pi R^4 \phi_0} \tag{34}$$

$$G' = \frac{3\Theta_0 M_0 \cos\delta}{2\pi R^4 \phi_0} \tag{35}$$

where ϕ_0 is the angular amplitude of oscillation and M_0 is torque amplitude.

Shear rate in the parallel-plate system (Figure 10b) is determined by the angular velocity Ω, the thickness of the sample layer, i.e., gap between the plates, h, and the distance from the center of the plate r. Because of the rotation kinematics, the parallel-plate geometry produces an uneven velocity field: the shear rate is at highest on the rim and zero in the center of the plate. Shear rate at the rim is

$$\dot{\gamma}_R = \frac{R\Omega}{h} \tag{36}$$

and shear stress calculated from the measured torque M. When the geometry is used in rotational mode for measuring non-linear properties, a correction procedure must be applied in order to overcome the error caused by the non-constant shear rate profile. Then the shear stress has the form

$$\tau = \frac{2M}{\pi R^3}\left(\frac{3}{4} + \frac{1}{4}\frac{d \ln M}{d \ln \dot{\gamma}_R}\right) \tag{37}$$

where the term in brackets is the correction factor analogous to the Rabinowitsch correction, which is applied in capillary rheometry for true wall shear rate (see Chapter *3.2*). Corrected viscosity is thus

$$\eta(\dot{\gamma}_R) = \frac{2M}{\dot{\gamma}_R \pi R^3}\left(\frac{3}{4} + \frac{1}{4}\frac{d \ln M}{d \ln \dot{\gamma}_R}\right) \tag{38}$$

For a Newtonian fluid the term in brackets yields 1 and shear viscosity is simply

$$\eta(\dot{\gamma}_R) = \frac{2M}{\dot{\gamma}_R \pi R^3} \tag{39}$$

In the dynamic operating mode in SAOS tests this problem is inexistent because of the minimal strain amplitude applied, and no correction is needed. In SAOS the storage- and loss moduli are determined as follows:

$$G'' = \frac{2h M_0 \sin\delta}{\pi R^4 \phi_0} \tag{40}$$

$$G' = \frac{2h M_0 \cos\delta}{\pi R^4 \phi_0} \tag{41}$$

From the moduli and the angular frequency, the complex viscosity can be calculated as shown in Equation 10.

Owing to the correction factor presented in Equation 37, the parallel-plate system can be used in the step-strain mode as well, although it is most commonly used for measuring the linear properties of the melts. Moreover, due to the non-constant shear field, the strain experienced by the fluid varies along the radius, and therefore for very strain-sensitive materials the result is a blur of all the strains measured. For such materials the cone-plate geometry may be a better option[3].

3.2 Capillary rheometry

For the pressure-driven flow, capillary rheometers with round-hole or slit die geometry are commonly used. In this study the measurements were carried out using round-hole dies with different length to diameter ratios (L/D). Polymer granules are fed into the pre-heated rheometer barrel (Figure 11). After filling the barrel and reaching the thermal equilibrium, the melt is extruded through a capillary die at a defined piston speed and the melt pressure is recorded in the barrel above the die entrance or within the die. Using a round-hole die, usually having a radius from 0.5 to 1 mm, mounting a pressure transducer within the die is not possible, thus the pressure must be measured before the melt enters the capillary.

Calculation based on capillary flow involves some assumptions and simplifications[15]: (i) the flow is fully developed, steady, and isothermal, (ii) no slip at the capillary wall; fluid velocity at the wall is zero, and (iii) the fluid is incompressible and its viscosity independent of pressure. Actually not all of these assumptions always hold for non-Newtonian viscoelastic fluids. The invalid assumptions for fully developed flow and no-

slip at the capillary wall are handled by different corrections as will be discussed briefly in this chapter[3].
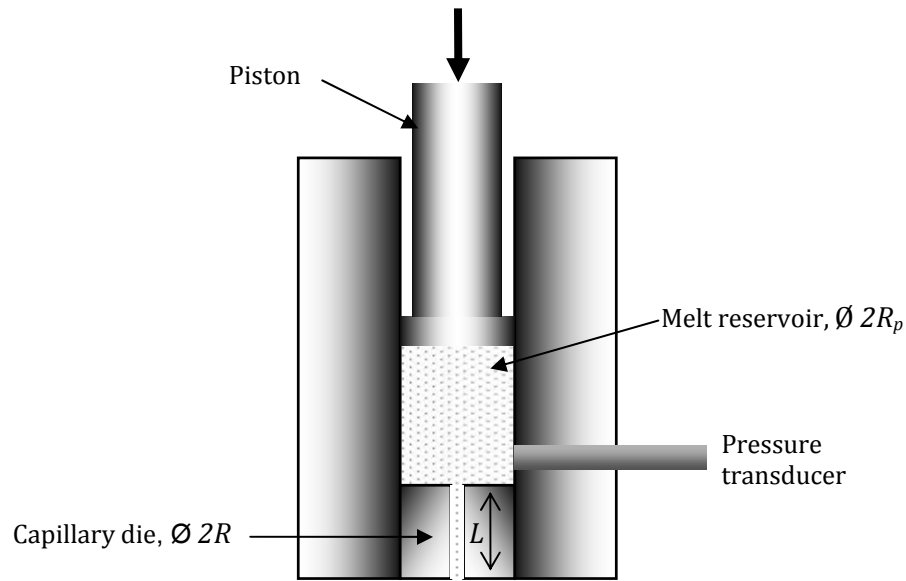

Figure 11. Principle of the capillary rheometer

The measurement is typically performed as a pre-set profile of alternating (either increasing or decreasing) shear rate. The volume flow rate in the barrel can be calculated as

$$Q = \pi R_p^2 V_p \tag{42}$$

where R_p is the barrel radius and V_p is the piston speed. From this and from the die dimensions the apparent shear rate, that is, the shear rate for a Newtonian fluid, at the capillary wall can be determined as

$$\dot{\gamma}_{wa} = \frac{4Q}{\pi R^3} \tag{43}$$

with R being the radius of the capillary. The apparent shear stress at the wall is calculated from the pressure (or actually from the difference between the atmospheric pressure and barrel pressure, Δp) measured in the barrel:

$$\tau_w = \frac{\Delta p}{2(L/R)} \tag{44}$$

For fluids with high molecular weight, elasticity causes disturbance of the flow pattern at the entrance of the capillary, where the fluid element stretches and accelerates through a sudden contraction. Similar effect, although much weaker, is observed at the die exit where the melt diverges. Re-circulating corner vortices have been observed in the entrance flow for some polymers, which has been related to a higher ratio of extensional to shear stress: the tendency to form a vortex increases with elasticity of the melt[1] (Figure 12).
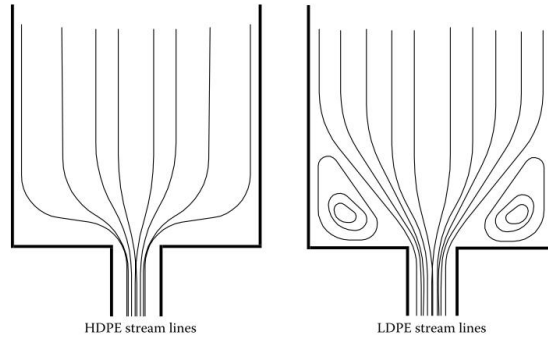
Figure 12. Melt stream lines in entrance flow at a contraction for a linear polymer (HDPE) and branched polymer (LDPE)[16]

Calculation in the capillary rheometry assumes a fully developed flow along the entire capillary length, thus omitting the end effects will lead to slightly overestimated pressure drop across the capillary. For achieving the true shear rate at the wall, τ_w, the extra pressure drop, Δp_e, arising at the entrance of the capillary die must be included in the calculation. The additional exit pressure drop at the capillary downstream is comparatively small and usually ignored. Correction is conventionally done through a Bagley correction procedure[17]: The measurements are repeated using at least three capillaries with the same diameter and different length. The Linear regression on the measured pressure vs. capillary L/D ratio plot is used to find the intersection on the pressure axis, which represents the pressure drop at the zero distance from the entrance, Δp_e (Figure 13).
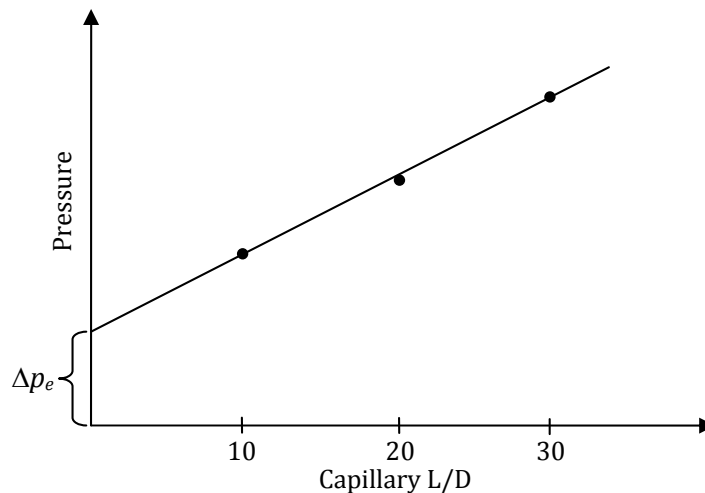
Figure 13. An example of Bagley plot with die length to diameter ratios 10, 20 and 30 at one measured shear rate.

For true wall shear stress the entrance pressure drop is subtracted from the total pressure drop across the capillary:

$$\tau_w = \frac{\Delta p - \Delta p_e}{2(L/R)} \tag{45}$$

A shortcut option for determining the entrance pressure drop is the use of an orifice die with a nominal length of zero. This procedure is discussed in detail and compared to the Bagley correction in Publication II.

21

A Newtonian, parabolic velocity profile in the capillary is assumed, although due to the shear thinning nature of polymer melts the profile is non-parabolic, resembling more a plug: the velocity is at highest in the centerline and zero at the wall, when the no-slip condition is valid. Thus the shear rate at the wall is at highest. The shape of the profile is defined by the power-law index n; the smaller its value, the more the profile deviates from parabolic. Shear rate at the wall can be calculated using a procedure known as the Rabinowitsch or Weissenberg-Rabinowitsch correction:

$$\dot{\gamma}_w = \left(\frac{3n'+1}{4n'}\right)\dot{\gamma}_{wa} \tag{46}$$

The local power-law index n' at each shear rate for any fluid is obtained by numerical derivation as a slope of the apparent shear rate vs. wall shear stress on a double logarithmic plot:

$$n' = \frac{d\log\tau_w}{d\log\dot{\gamma}_{wa}} \tag{47}$$

The most straightforward way of performing the Rabinowitsch correction for experimental data is through a polynomial fitting on $\log\tau_w$ vs. $\log\dot{\gamma}_{wa}$. Differentiation of the polynomial equation in terms of each $\log\dot{\gamma}_{wa}$, gives the local power law index n' for each measured shear rate. For power-law fluids the slope of the polynomial fitting curve remains constant, thus $n' = n$. Viscosity corrected for both entrance pressure drop and the non-Newtonian flow profile is then

$$\eta = \frac{\tau_w}{\dot{\gamma}_w} = \frac{R(\Delta p - \Delta p_e)}{2L[(3n'+1)/4n']\dot{\gamma}_{wa}} \tag{48}$$

Correction for the entrance pressure drop and plug-like flow in pressure-driven contraction flow are well-known procedures in capillary rheometry. Nevertheless, their significance is sometimes overlooked and the data handling phase skipped. This can perhaps be justified for quality-control purposes where the only goal is to ensure the consistence of a polymer grade between different polymerization batches, and the control is done comparing the test results obtained for different batches always using an identical test procedure. When the aim is to examine the true rheological behavior of polymers and the reflections of molecule-level properties, such as chain architecture or molecular weight distribution to the rheology, it becomes extremely important to follow careful experimental procedures minimizing the influence of all external factors, and also to perform all the possible corrections that eliminate the errors caused by the above discussed assumptions. This is equally important when measured data is used for process simulation purposes: the models for flow simulation give good predictions only if the measured data used to form the data bank for each material is exact and correct.

The general no-slip assumption of classical fluid mechanics dictates that the melt adheres to the capillary or slit wall. However, for some polymers, when a critical shear stress is exceeded, the melt starts to slip along the wall, thus the fluid velocity at the capillary wall is nonzero and the true shear rate smaller than in a no-slip case. The wall slip can be determined by performing parallel measurements with dies having a different diameter but the same length-to-diameter (or radius) ratio: if the plot of apparent shear rate vs. 1/R at constant wall shear stress gives a horizontal line, no slip occurs. If the curve is linear with a positive slope, slip occurs, and the slip velocity at the wall can be calculated from the slope, according to the procedure proposed by Mooney[18].

Entrance pressure drop in capillary rheometer with either round-hole or slit die can be used to evaluate the extensional viscosity. Contraction flow analysis method is based on the assumption, that the pressure drops due to shear and extensional deformation

can be calculated separately and their sum is the total pressure drop. Additionally the general assumptions of capillary rheometry are applied in the contraction flow analysis as well. Cogswell[19] and Binding[20] analyses are the most popular techniques for estimating the extensional viscosity from the capillary rheometry data. The first one is discussed in more detail and compared to extensional viscosity in uniaxial extension in Publication IV.

3.3 Slit rheometry

Instead of a round-hole capillary, a wide $w \times h$ slit can also be mounted on a capillary rheometer to measure rheological properties in pressure-driven flow (Figure 14). The calculation presumes that the slit is infinitely wide, which in practice can be assumed with a good accuracy when $w \geq 10h$. When this is the case, the effect of the edges can be ignored. The main advantage of a slit die is its flat wall geometry that enables measurement of pressure directly in the slit where the flow is fully developed, thus making exact determination of pressure profile possible. For this reason, the correction of the entrance pressure drop is unnecessary. Slit dies are, however, more difficult to assemble and to disassemble. In addition, cleaning of the slit edges requires more effort: possible remnants of burned or charred melt at the edges can reduce the die dimensions and thus cause a computational error[21]. Another source of error possibly occurring with a slit die is the so called hole-pressure error, related to the normal forces present in the flow of viscoelastic fluids over a discontinuity of the pressure transducer bore. Slit constructions and hole pressure error can also be used for determining the normal stress differences by means of transverse pressure transducer: the hole-pressure error can roughly be approximated to be one third of the first normal stress difference for shear-thinning fluids[22].
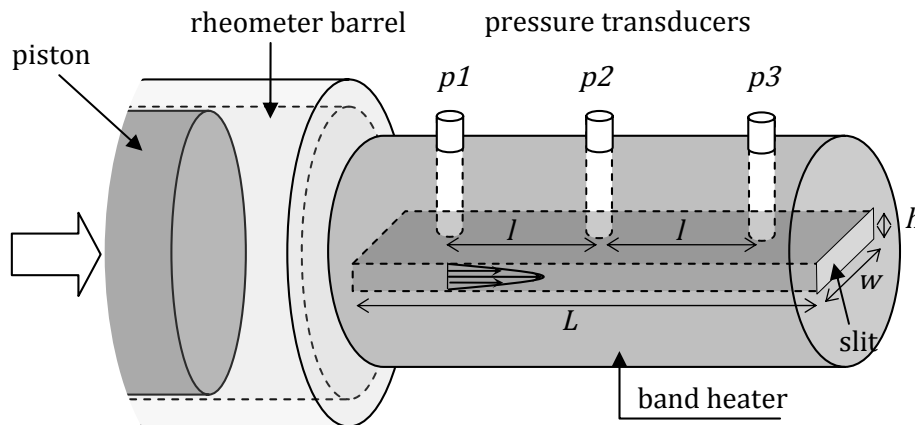

Figure 14. An illustrational drawing of a slit die rheometer

Shear stress on the slit wall is

$$\tau_w = \frac{h}{2}\frac{\Delta p}{l} \tag{49}$$

where $\Delta p = p1 - p2 = p2 - p3$ if the pressure profile is linear, that is, if neither pressure dependent viscosity nor viscous heating cause any curvature to the pressure

profile across the slit. In capillary geometry these possible non-linearities can be observed as an upward (pressure dependence) or downward (viscous heating) curvature of the Bagley plot for end corrections[22,23]. The shear rate for a Newtonian fluid (apparent shear rate) in a rectangular slit is

$$\dot{\gamma}_{wa} = \frac{6Q}{h^2 w} \tag{50}$$

For shear-thinning polymers the correction for the non-parabolic velocity profile must be performed analogously to the Rabinowitsch correction for capillary die calculations:

$$\dot{\gamma}_w = \frac{6Q}{h^2 w} \left(\frac{2n'+1}{3n'} \right) \tag{51}$$

where

$$n' = \frac{d \log \tau_w}{d \log \dot{\gamma}_{wa}} \tag{52}$$

Shear viscosity at the slit wall is then

$$\eta = \frac{\tau_w}{\dot{\gamma}_w} = \frac{h \Delta p}{2l[(2n'+1)/3n']\dot{\gamma}_{wa}} \tag{53}$$

A simpler, yet reasonably accurate alternative for accounting for the non-Newtonian velocity profile has been proposed by Schümmer and co-workers[24,25], and developed further by Giesekus and Langer[26]. This procedure is based on estimating the shear rate and viscosity at radial distance r (for circular geometry) or vertical distance y from the flow slit center (for a rectangular slit), where the apparent shear rate equals the true shear rate. Hence, considering that under fully developed conditions the apparent shear rate, as well as the shear stress, varies linearly with radial position, one obtains

$$\eta(x^* \dot{\gamma}_{wa}) = \eta_a(\dot{\gamma}_{wa}) \tag{54}$$

Factor $x^* = r/R$ for a circular capillary, where R = radius of the die, and for a slit geometry $x^* = 2y/h$, where h is the slit height[26]. Apparently, when $n = 0.36 - 1.2$, x^* varies by only a small amount, so that a representative value of x^* may be chosen for most materials with very little loss in accuracy. For rectangular slit this approximation is given as[1]

$$x^* = \left(\frac{2n+1}{3n} \right)^{n/(n-1)} \approx 0.79 \tag{55}$$

and for circular capillary as

$$x^* = \left(\frac{3n+1}{4n} \right)^{n/(n-1)} \approx 0.83 \tag{56}$$

The Schümmer approximation is valid for a true shear stress $x^*\tau_w$. It shifts data only horizontally (to the left) and can be applied to single points.

3.4 Rheological measurements with polymer processing machines

In order to achieve data at high shear rates relevant for injection molding, performing rheological measurement using a capillary or slit die connected to an injection molding machine is an attractive option. This way the measurable melt experiences similar thermal and shear history as in actual processing, and thus the results from such measurements can be assumed to best serve for the evaluation of processability of a polymer. Moreover, use of processing machines as rheometers often enables achieving higher deformation rates which are out of the measurement range of a regular capillary rheometer.

Continuous in-process experiments can be separated by means of the melt flow through the measurement device: In in-line measurements the entire melt stream passes through the measurement unit. By-pass on-line experiments are referred to, when the measurement is only made for a part of the melt stream that is directed to by-pass the process stream through the meter. In recycled on-line measurement, the by-passed melt stream is directed back to the process line after measurement[27]. In many works where the plasticizing is done by an injection molding machine and the pressures are recorded in the die fixed on the mounting table, the term "in-line measurement" is used[28,29]. One can, however, also understand the in-line measurement as an experiment that is carried out simultaneously with actual processing. In the case where a slit or capillary die is mounted to an injection molding machine, it replaces the mold, thus no actual molding can be done at the same time with such experiments and the term "in-line" must be understood a bit differently.

Rheological measurements can be accomplished by means of a die, either circular or rectangular, where the pressure and temperature are recorded by transducers mounted on the die wall and/ or entrance. Such a measurement unit can be connected to either an extruder or an injection molding machine. In case of extrusion, continuous screw rotation causes the flow through the die, and therefore the flow rate cannot be calculated simply from the screw rotation speed and barrel dimensions, but the characteristic flow resistance of the die has to be considered as well[1]. The accurate flow rate can be determined by collecting the extrudate over a specified time period, weighing it, and using the melt density value of the material to convert the mass-flow rate to volume-flow rate[27]. After this the shear rate corresponding to the screw rotation speed can be calculated. In an injection molding machine the calculation of the flow rate is more straightforward; injection through the die occurs shot-wise by a rapid movement of the screw at a pre-determined speed and over a set distance, and the flow rate can be calculated using Equation 42. However, especially at low injection pressure, one has to consider the possible leakage flow of melt from the nozzle, backwards along the screw, which can reduce the theoretical flow rate[30].

High shear-rate viscosity has been examined by circular capillary die specially designed and built in-house[31,32,33]. Tailor-made rectangular slit dies and hyperbolically converging and diverging planar dies have also been used for extensive examination of shear and elongational properties of polymers[34] utilizing Cogswell and Binding analyses for determining the apparent extensional properties. At the moment a commercial device with a wide slit[30] compatible with injection molding machine also exists. The slit die experiments using an injection molding machine as a rheometer are discussed further in Publication VI.

3.5 Extensional rheometry by counter-rotating drum device

Uniaxial extensional flow, also called simple extensional flow, is a standard rheological flow like simple shear. When extensional flow properties of polymer melts are of interest, it is the most common flow type measured. Different experimental set-ups have been developed during the last decades. Different devices based on same principle; stretching the sample strip between counter-rotating drums at a constant rate (Figure 15), have been developed and commercialized. One of such designs, Sentmanat Extensional Rheometer (SER)[35], was used in this study. A similar design is the TA extensional viscosity fixture[36], with the difference that one drum remains stationary while the other one rotates around it. Probably the first device of this type was the fiber windup fixture[37] where the other end of the sample strip is stationary, and the other end fixed on a large-diameter drum which rotates around its axis.
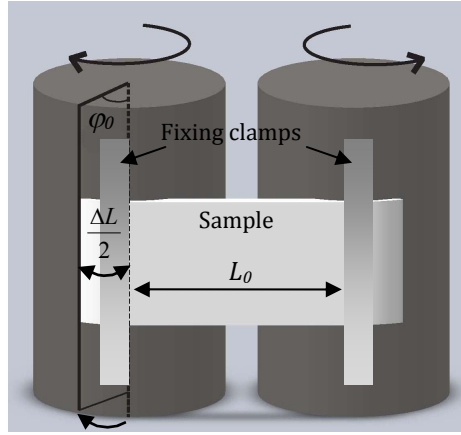

Figure 15. Operation principle of the SER counter-rotating drum device. L_0 is the initial length of the sample stretching zone, ΔL is the change in sample length ($\Delta L/2$ at both sample ends) due to initial drum deflection angle φ_0.

Usually the experiments are made in un-steady start-up extension (transient extensional viscosity). The chain architecture of a polymer becomes apparent in the non-linear phase of the start-up test: long-chain branched polymers typically exhibit strain hardening and linear polymers strain thinning, as was shown in Figure 7. Attainment of the steady-state flow in extension is in general difficult. With SER the limiting factor for this is often in practice sample necking and rupture. If the drums are allowed to rotate over one full revolution, 360°, the sample strip starts to wind up on the clamps, which causes an unexpected peak in the transient viscosity curve[38]. Therefore the maximum drum rotation angle can also be a limiting factor for achieving steady-state flow. In our tests the fixing clamps were not used. The Hencky strain rate at constant drum rotating speed Ω is

$$\dot{\varepsilon}_H = \frac{2\Omega R}{L_0} \tag{57}$$

with R being the drum radius and L_0 being the initial length of the stretching zone, that is, the gage length between the fixing clamps, 12.72 mm. The transient extensional viscosity can be calculated as

$$\eta_E^+(t) = \frac{\sigma_T}{\dot{\varepsilon}_H} = \frac{M}{2R\dot{\varepsilon}_H A(T,\varphi_0)exp[-\dot{\varepsilon}_H t]} \tag{58}$$

where σ_T = tensile stress, M = momentum, t = time, and the cross-sectional area of the sample as a function of both drum deflection angle and temperature, $A(T, \varphi_0)$ is taken into account as follows:

$$A(T, \varphi_0) = \frac{L_0 wh}{\left(L_0 + \frac{4\pi R \varphi_0}{360°}\right)} \left(\frac{\rho_S}{\rho_M(T)}\right)^{2/3} \tag{59}$$

Here, w = sample width, h = sample thickness, φ_0 = initial drum deflection angle, ρ_S = sample density at solid state, and $\rho_M(T)$ = sample density at melt state at test temperature T. The initial deflection angle of the drum means the drum rotation needed in the pre-heating phase in order to avoid sagging of the sample before the actual test. Temperature correction, on the other hand, takes into account the thermal expansion of the polymer. Correction procedures for both of these effects are presented in detail in Publication IV.

Gravitational sagging of the sample during the heating prior to the actual stretching is a problem causing serious inconsistency between the results. Besides using pre-stretching and taking the initial deflection angle into account in the calculation of sample dimensions, a very different and interesting way has also been used to overcome this: an MIT research group performed uniaxial extension experiments on dilute polymer solutions in a weightless environment at the International Space Station to eliminate the effects of gravity[39]. This method is naturally out of reach for ordinary laboratories, but tests in a liquid of the same density as the tested polymer can in principle be used: in fact, the 2nd generation design of SER[40] enables immersion of the testing system into a liquid. If a floating liquid is used, proper fixing of the sample is essential to avoid slipping or loosening from the test drums. Recently, uniaxial extensional viscosity measurements by SER have also been numerically simulated: in simulations an uneven necking close to the attachment points onto the drums was observed[41]. Necking causes an uneven strain distribution along the sample strip, and thus the locally observed strain rate also deviates from the pre-set Hencky strain rate.

3.6   Other devices for uniaxial extension

In addition to rotating drum devices other types of designs for uniaxial extension exist: Meissner type rheometers, of which RME (Rheometrics Melt Extensiometer)[42] is a commercialized version, involve stretching of the polymer strip by rotating belts or clamps in a horizontal position, where the sample is supported by oil bed or inert gas flow. In MTR (Münstedt Tensile Rheometer)[43] the sample is in a vertical position in an oil bath, which prevents sagging and ensures an accurate temperature control and distribution in and around the sample. In both these devices the actual strain rate is observed by an external device: in RME a video camera recording is used during the test, and in MTR the length of the sample is observed electro-optically. In filament stretching rheometer (FSR), originally developed for low-viscous solutions but later revised also for polymer melts[44], the sample mounted between cylindrical plates is stretched vertically. The strain rate at the center of the sample remains constant and the extension is purely uniaxial. Another advantage of FSR over SER, MTR and RME is the capability of measuring the extensional viscosity of less-viscous fluids.

A melt spinning device, such as Göttfert Rheotens[45], is an approximate test method where the polymer melt is extruded from a capillary and the filament is spun on a roll downstream. Here the melt is subjected to the temperature of the environment, thus the flow is non-isothermal. However, at high spinning rate the cooling effect can be assumed to have a minimal effect. The spinning rate is determined by the tensile drawdown force, thus the strain and strain rate experienced by the melt strand varies along its length by changing thickness. Although the true uniaxial extensional viscosity cannot be measured

directly due to uncontrollable variables; non-uniform temperature and strain, the device is useful in determining the melt strength[46], which is an important measure when evaluating the polymer's eligibility for example to be processed by fiber spinning[47].

Despite the variety of different experimental settings for uniaxial, biaxial, and planar extension, a reliable measurement is still not a simple task and each technique has certain limitations[48]. Results between devices based on different principles and even between different laboratories, due to their sample preparation technique, can differ from each other. Different types of tensile stretching devices were compared together and with converging flow analysis in the study coordinated by the National Physics Laboratory (NPL)[49]: Especially the steady-state or maximum values in start-up extensional flow varied highly between the experiments. However, some agreement was found in overall comparison between uniaxial extension techniques and contraction flow analysis. NPL has put some effort on creating framework for standardizing the experimental procedure for defining the transient extensional flow properties for polymer melts[50] which is now stated in ISO 20965:2005.

3.7   Sample preparation and treatment in rheological measurements

Rheological properties of polymers are sensitive to many external factors, such as humidity, heat, or impurities. Numerous factors arising from improper sample handling or preparation of experimental setting can cause discrepancy and poor reproducibility of the results, or in worst case rough misinterpretation of the rheological behavior of the examined material. Further, poor design of the measurement device or limitations dictated by solely constructional or practical reasons can give erroneous results, which require post-processing for extracting true material properties of the output data.

Thermal stability of polymer melts is an important issue to be considered in processing as well as when performing rheological characterization. Some polymer grades are very sensitive to excess heat and/or shearing, showing chain scission and hence decrease of molecular weight, which is reflected in the properties of final products, for example, as color changes and weaker mechanical properties. Thermal degradation is pronounced in the presence of oxygen, and therefore parallel-plate and cone-plate rheometer measurements are often conducted in a protective gas – usually nitrogen – atmosphere. Viscosity is very sensitive to changes in molecular weight, and the degradation can be observed as decreasing viscosity in a time sweep experiment at constant shear rate or angular frequency. However, some polymers can also start forming cross-links due to the excess heat, and show a drastic increase in viscosity. In dynamic tests storage modulus reveals changes in elasticity due to cross-linking clearly, as demonstrated for example for a metallocene-catalyzed narrow-MWD LDPE (Figure 16). In the experiment the polymer remained stable over the entire measurement time of approximately one hour when the protecting nitrogen atmosphere was used during the experiment, whereas without nitrogen atmosphere the oxidation and cross-linking started already after few minutes.
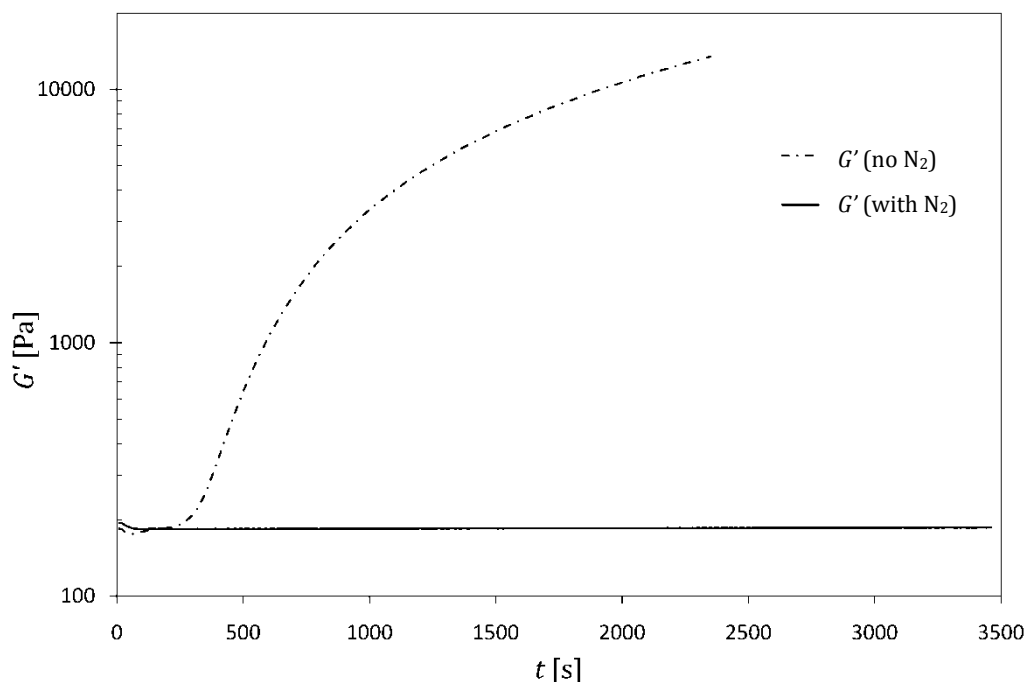
Figure 16. Time sweep for an LDPE at 230 °C. The solid line represents the storage modulus measured under protecting nitrogen atmosphere, and the dashed line is storage modulus from an identical measurement but without the protecting gas atmosphere.

The possibility of thermal degradation should also be taken into account when samples for rheological tests are prepared. For some measurements, such as the extensional viscosity measurements by SER, sample strips must be prepared beforehand by hot pressing the resin into thin sheets. It is important to use enough shearing and heating to avoid inhomogeneities of the sample, such as granular boundaries or thickness variations, while making sure that the sample preparation process is gentle enough to maintain the original properties of the material.

Another very important factor is the effect of moisture in polymers. Some types of polymers, e.g. polyamides and polycarbonate, absorb humidity from the surroundings very easily. The water molecules act as plasticizers in the polymer, intruding between the molecules and lowering the viscosity. Therefore a careful drying, following the polymer supplier's recommendation, must be done before any rheological characterization, as well as before melt processing. Moisture absorption can happen very fast, already while moving the test material from a drying chamber to the measurement device. Some thermal degradation can also happen during the sample loading, so already the first measured data can be corrupt[1].

In some cases human factors can have an influence on the measurement reliability: a good example is the capillary rheometer experiment, where the test material is fed and compressed by hand. The force used in doing this affects the compression level of the melt in the barrel and can lead to slight differences in the pressure recorded at the lower end of the barrel. Similarly, in cone-plate or parallel-plate measurements, a careful trimming of the sample around the rim is important: too much melt outside the lower plate of the system causes a slight addition to the measured torque signal[51], but even a larger error arises, if the gap between the measurement heads is not completely filled – the same error that is caused due to edge fracture[15]. For especially sensitive polymers the time used for sample loading and preparations before the experiment is started may also affect the results through variations in moisture absorption or thermal history. In order to be able to utilize measured rheological data for modeling purposes reliably, a uniform, careful measuring procedure for all the rheological properties should be followed.

4   ROLE OF RHEOLOGY IN POLYMER PROCESSING

Shear and extensional rheology play a critical role in processing. For example, shear thinning is a property that is required to enable some processing methods: if polymer melts did not show shear thinning, much higher injection pressures would be needed for filling the mold cavity, and molding of very small and thin parts would probably not be possible at all. Other processes, such as extrusion, are also enabled by shear thinning. Many polymer-forming processes involve both shear and extensional deformation types. Shear flow, however, is easier to produce in laboratory conditions and thus it is the most commonly used mode for characterizing flow behavior. Generally, extrusion and injection molding are processes, where shear deformation dominates. For secondary shaping processes, such as fiber spinning, blow molding and film blowing, by contrast, extensional viscosity gives a more important indication of the polymer processability. In the following, the role of rheology in the above mentioned melt processes is discussed, the main emphasis being on the rheology in injection molding, and the use of rheological data in injection molding simulation.

4.1   Rheology in injection molding

Rheology and thermal properties of the polymer determine the ability of the melt to fill the mold cavity and form a solid, un-warped part of a desired form. Knowing the rheological behavior of the polymer is important already in the mold-designing phase. It allows sizing the mold dimensions properly to avoid short shots or other filling problems. In the packing and cooling phase, the characteristic relaxation spectrum of the polymer contributes to the amount of residual stresses and orientations in the molded part, along with the thermal properties of the polymer and the cooling speed. Residual stresses directly affect the mechanical properties of finished parts and can lead to shrinkage and warpage during and after the cooling phase. The following indicates the importance of the knowledge of rheological behavior of polymers for successful injection molding and its computer-aided modeling. Whilst the focus here is on the polymer melt flow in the runners, gates and cavity, various other factors need to be considered as well for the thorough management of the process.

In injection molding the polymer is plasticized in a heated barrel by a rotating screw. During plasticizing the screw moves backwards simultaneously accumulating plasticized, homogeneous polymer melt in front of its tip for a shot volume for filling the mold cavity. When a sufficient amount of melt has been homogenized, it is injected to the mold through the gate with a rapid forward movement of the screw. Once the melt enters the mold it immediately starts to cool down, which leads to a formation of an oriented frozen layer or "skin" on the wall and a less-oriented core. The final filling of the mold is done in the packing phase, where the slow injection ensures the complete filling and compensates for possible shrinkage of the part during and after the cooling. While the part is cooling in the mold, the screw retracts, plasticizing material for the next cycle.

4.1.1 Filling phase

The melt proceeds in the barrel during plasticizing by a drag flow mechanism, and in runners, as well as in the mold cavity, by pressure-driven flow. In the rapid, isothermal tube flow the orientation of the molecules at the wall cause a non-parabolic flow profile: The shear-thinning property of polymer melts turns the velocity profile to more plug-like, so that the outer part closest to the skin experiences the highest rate of shearing. This means that the maximum strain in the tube flow occurs at the tube wall, but the average strain for the total flow in the tube is far smaller[1,52]. Due to the cooled mold cavity, the flow in the mold is non-isothermal: the skin forming on the outer surface has the most frozen-in orientations, while the core that stays molten for a longer time, remains less oriented.

The mold cavity is filled by pressure-driven flow and during the filling stage the advancing flow front in the cavity has a fountain-flow pattern (Figure 17) where the melt "folds backwards" to the mold wall and forms the solidified outer layer, the afore-mentioned skin. The fountain-flow front is generally semispherical in shape; however, numerical simulations in a recent study showed that increasing melt elasticity changes the flow profile towards bullet-like. In addition to the viscoelastic properties, the flow front is also affected by the flow rate and the geometry; a high flow rate increases the bullet-likeness of the flow front, and planar flow geometry produces more bullet-like flow front compared to an axisymmetric flow channel[53].
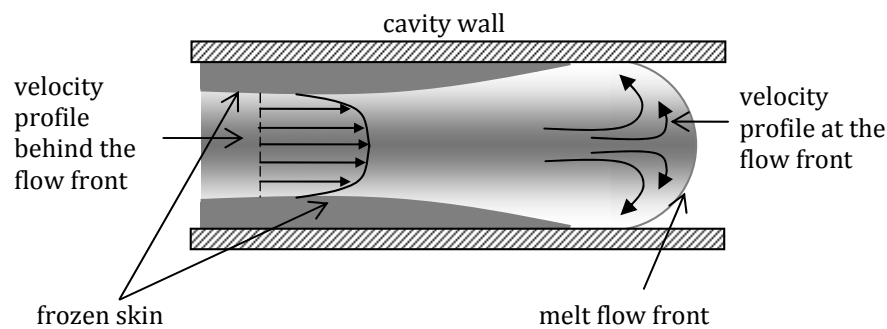

Figure 17. Representation of fountain-flow in the mold cavity

In the filling phase, especially at the mold gate, the rapid screw-forward movement causes very high shear rate and high pressure. The shear rate, depending on the channel profile and dimensions, can be as high as 10^5 s^{-1} and the pressures exceeding 100 MPa are not uncommon[52]. As viscosity is an exponential function of pressure, the pressure dependence of viscosity may become important at this point for some materials. The melt is at high temperature in the filling phase, and some viscous heating also occurs due to friction. This increases the melt temperature even more and thus lowers the viscosity. Therefore viscous heating has been considered to partly counteract the effect of pressure that tends to increase the viscosity[54]. However, a more recent study[55] speculated that at extremely high pressures the effect of pressure would overrule the effect of temperature increase on viscosity and therefore the effect of viscous dissipation and the increasing pressure could not be assumed to cancel each other.

At the gate the melt flows through an abrupt contraction, and the flow streamlines converge causing acceleration of fluid particles and thus – in addition to shear – also extensional deformation. The proportion of the extensional deformation increases with increasing elasticity of the melt and thus for melts with high elasticity, the extensional flow component has a more significant effect on the overall pressure drop[56].

Both above-mentioned factors affect the correctness of the estimation of needed injection pressure: rising pressure increases the viscosity of the melt, which in turn

requires higher injection pressure in order to fill the cavity. For melts with a high elastic contribution the larger pressure drop at contractions increases the need of injection pressure compared to less-elastic polymers. Extensional properties as well as the pressure dependence of viscosity are dependent on molecular structure and chain architecture[57], and the significance of their contribution to the overall pressure must therefore be treated separately for different types of polymers.

4.1.2   Packing phase

Once the mold is volumetrically filled, the process is switched from velocity-controlled injection phase to pressure-controlled packing phase. The purpose of the packing phase is to compensate for the shrinking of the part due to the solidification and (for semi-crystalline polymers) crystallization that continues after the part has been removed from the mold. If the packing pressure or packing time is insufficient, part dimensions can continue distorting (warpage) and shrinking even days after molding. Unlike the filling phase, the packing phase is characterized by flow at low temperature and at low shear rate, before the melt finally solidifies. When the mold gate is sealed due to melt solidification, the packing pressure ceases to affect and the part has reached its final density. The solidification point, the point at which viscosity gets high enough to cease flowing, is described in injection molding simulation as "no-flow temperature" or "transition temperature"[58].

4.2   Significance of rheology in injection molding simulation

Using simulations in designing the injection molding part, mold gating and cooling, and the process, can be of great aid. With correctly performed simulation it is possible to reduce trial and error, time-to-market of the products, re-adjustments of the mold and process parameters, and molding material waste. Starting with a computer aided design (CAD) model of the part to be molded, material characteristic data of the molding resin are needed as input parameters; rheological properties are needed for flow behavior prediction, thermal properties for the cooling analysis, pressure-volume-temperature (pVT) and mechanical properties for modeling the packing phase and predicting post-ejection shrinkage and warpage.

Finite element method (FEM) calculation is the prevailing method to solve the numerical problems in fluid flow, as well as in several other types of problems, for example, in solid mechanics and heat transfer[59]. First attempts to simulate the injection molding process were done in the 1950's, and the first models used were 1-dimensional models. In order to be able to simulate the melt flow in a complex cavity with a simple 1-dimensional approach, the geometry had to be deconstructed and laid flat into different components, in which the flow analysis is performed separately. After this the components were re-joined to a complete model and adjusted for the equal pressure drop and total flow rate[60].

The 2.5D approach offers a more sophisticated model, which is useful for modeling thin-walled mold geometries and when the fluid has a high viscosity, as polymer melts do. 2.5D simulation uses either mid-plane or surface models (Figure 18 a, b). In the mid-plane model an arbitrary central plane of the part is meshed and the thickness is given to create the "three-dimensionality". However, the simulation with a mid-plane model is not a real 3D simulation. In the surface model the part's outer surface is meshed, and the mesh elements on the opposing surfaces are aligned and matched to represent an actual three-dimensional part. The model preparation time for converting the commonly used solid CAD models to a surface model is much shorter than with the mid-plane model,

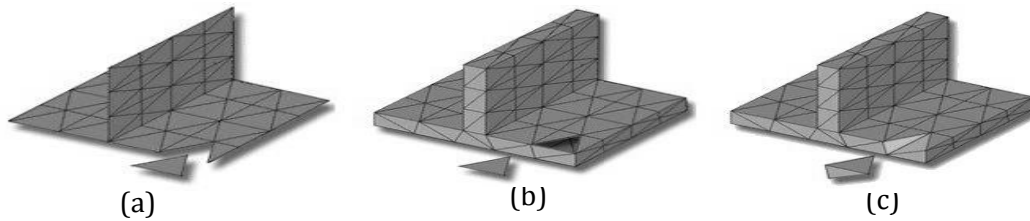and in injection molding simulation the surface model is presently the most commonly used[60].

Figure 18. 2.5D models; (a) mid-plane, (b) surface, and (c) a true 3D model with tetrahedral elements.

If the part to be modeled is not thin-walled and relatively simple, a surface model does not provide accurate approximation of the flow geometry. Simplifications related to approximations used in the 2.5D modeling do not allow for correct prediction of flow in junctions or abruptly changing cross-sections, nor around special parts of the mould, such as ribs, bosses, and corners. Neither does it work with thick-walled parts. For such cases a true 3D model with tetrahedral volume mesh elements (Figure 18c) should be used. This increases the calculation time dramatically but has nevertheless become manageable with the ever-increasing computing capacity of modern computers. Presently there are still unsolved issues regarding its computing flexibility and efficiency, thus the surface model still remains the prevailing mesh type in common injection molding simulations[60].

4.2.1   *Calculation basis for polymer melt flow in 2.5D simulation*

For modeling polymer melt flow in injection molding, the conservation equations of mass, momentum and energy must be satisfied, simultaneously fulfilling the constitutive equations for material functions and the boundary conditions for the flow.

Conservation of mass dictates that the mass flow rate in must equal the mass flow rate out. If incompressible fluid is assumed, the same can readily be applied to the volume flow rate, but for compressible flow, which is assumed in injection molding simulation, a variable density, defined by the pVT parameters, needs to be included. The solution of the conservation equation of momentum (motion) gives the velocity field at a given point in time and space. For modeling the fluid flow in non-isothermal conditions, the law of conservation of energy must also be fulfilled. It states that the rate of heat loss of a body is proportional to the difference in temperatures between the body and its surroundings, and determines the cooling of the polymer melt in contact to the mold wall[3,59].

For a complete description of fluid flow in injection molding, material constitutive equations and boundary conditions are required. In injection molding simulation, the rheological constitutive equations for generalized Newtonian fluid (GNF) flow are used. As extensions of Newtonian constitutive equation, GNF equations are capable of describing the viscosity as a function of shear rate, as explained in Chapter 2.4 where common GNF equations are given. However, GNF equations are not able to describe the viscoelasticity, hence they cannot be used to define the normal stresses in polymer fluid flow[3].

The number of boundary conditions in injection molding problems is relatively small and depends on the type of flow problem and geometry. The first boundary condition for the flow is *no-slip at the wall*, meaning that velocity of the fluid at the wall is the same as the velocity of the wall. Usually the walls are not moving, thus *v=0*. The second boundary

condition states *symmetry around the central plane*: If the flow has a plane of symmetry, the velocity has its minimum or maximum on that plane, and its first derivative on the plane is zero. The symmetry condition is also applied in the heat transfer phenomena related to cooling: the temperatures on both sides of the center plane are assumed equal. Another boundary condition needed for modeling of cooling is the heat transfer coefficient between the polymer melt and the mold wall. Further boundary conditions can be identified according to the flow problem at hand[3,59].

4.2.2   Simplifying assumptions

The above requirements lead to highly non-linear equations, and in order to be able to solve them unambiguously, some general assumptions must be made in numerical simulation. In order to enable a smooth simulation within an acceptable time, simplifications are done regarding the material properties, the flow geometry, and the governing balance equations involved in the process[58].

For a reliable 2.5D simulation one prerequisite is small thickness compared to the flow length. Using the assumption $h \ll L$ and ignoring the fluid inertia, the momentum equations for the flow velocity field are simplified to a form called the Hele-Shaw approximation, which was first applied to solve flow problems in injection molding simulation in the early 80's[61]. The fountain flow in the mold cavity cannot be modeled, as only the unidirectional flow streamlines are taken into account. For the same reason, the converging flow in junctions and changing cross-sections is ignored[62,63].

The first simplification related to the rheological properties is the fact that the polymer melt is treated with GNF flow equations, thus the elastic effects are ignored. The viscosity models used in injection molding software are generally of Cross or Carreau type. The Carreau-Yasuda equation has one freely fitted parameter more and thus provides the best fit for the widest variety of shear thinning polymer melts. However, the choice of the viscosity model does not seem to play a very critical role in the overall simulation accuracy[14]. Use of viscoelastic constitutive equations would multiply the required calculation time, especially for complex geometries often dealt with in injection molding. Besides, none of the existing viscoelastic constitutive equations is able to predict complex flow for any given geometry universally, but merely describe a certain, simple flow. Due to these complications, no commercial flow simulation code with true viscoelastic constitutive equations exist[62], although several case-specific simulation experiments using viscoelastic models have been conducted, for example for analyzing the cavity filling[63,64], fountain-flow instabilities[65], and residual stresses, shrinkage and warpage[66,67]. Secondly, the increase of viscosity with increasing pressure is most often ignored, although compressibility of the polymer melt is taken into account through the pVT parameters for enabling the calculation of the packing phase. Thirdly, extensional deformation occurs at gates, junctions and converging cross-sections. Normally, however, only shear viscosity of polymers is used to describe the flow, with the simplification that the main type of the deformation occurring in mold filling is shear[68]. These points are discussed further in the following.

4.2.3   Pressure dependence of viscosity and other rheology-related challenges in injection molding simulation

Melt viscosity increases with pressure, when the decreasing free volume in the polymer structure causes more interaction between the molecule chains. The effect of pressure on melt viscosity can be ignored when the polymer process does not require high pressure operation. However, in injection molding high pressure is often involved. The significance of the pressure effect on the viscosity depends on the polymer's

molecular structure and melt temperature, as explained in Chapter 2.1.5. Apparently pressure dependence becomes relevant for the accuracy of injection molding simulation only above a certain pressure level: one estimation of the critical pressure limit, presented in literature, is 100 MPa[69], although for certain polymers the pressure obviously affects the viscosity significantly already at much lower pressures (Publication III). Ignoring the pressure-induced viscosity increase in simulation can lead to under-predicted nozzle pressure and over-predicted pressure inside the cavity[70]. The pressure coefficient can be introduced to a GNF viscosity model through a WLF type relationship, as for example in Cadmould®[71] and Autodesk Moldflow®[72] injection molding simulation software. In fact, the option for taking pressure dependence of viscosity into account has existed in flow simulation codes for over twenty years now[73]. However, it still seems to be very seldom characterized in rheological tests and therefore, for most materials, the pressure dependence parameter is missing in the software databases.

For flow in a narrow, uniform gap without any obstacles disturbing the flow, polymer melt exhibits mostly shear flow, and an accurate prediction can be achieved with purely viscous flow models for shear viscosity. However, viscoelasticity manifests itself as a disruptive flow pattern at each discontinuity in the mold cavity, in runner junctions, at varying cavity gap height, or at the gate: When the melt flows from a larger to a smaller cross-section, it stretches through the contraction experiencing extensional deformation. This causes additional pressure loss at contractions and junctions, often referred to as "juncture loss"[69]. Its significance regarding the overall pressure in the process depends on the viscoelastic properties of the melt and thus varies for each material. In one study extensional properties of LDPE were modeled using a Carreau-Yasuda equation modified for extensional viscosity to simulate the contraction flow at the capillary entrance[74]. The model does not capture true viscoelastic behavior, but a reasonable description of the extensional deformation estimated by the Binding method was established. Likewise, better accuracy in injection molding simulation – compared to the use of a mere GNF model – was also achieved in another study using a dualistic viscosity model with both extensional and shear deformation[75].

A recent study[58] summarizes the state-of-the-art of the injection molding simulation, concentrating mainly on the issue of shrinkage and warpage simulation. It also points out the problem of a different flow situation in conventional rheological experiments compared to the actual injection molding process. As briefly discussed in Chapter 3.4 and in Publication VI, some studies on rheological experiments in injection molding conditions have been done: especially the high shear rate viscosity data has been measured in-line, using a die fixed to a stationary mounting plate of an injection molding machine[31,32,33]. Modeling the phase change is another great challenge in simulation: rapid change in viscosity due to solidification cannot be predicted by any GNF flow model, and the solidification is simply described by a no-flow temperature, or a transition temperature, at which the melt fully ceases to flow[58]. Neither do the commonly used viscosity models describe the yield stress behavior at low shear rates, typical for highly filled and rubbery polymers. Further, as specified above, more accurate pressure prediction in injection molding simulation could be achieved if pressure dependence of viscosity and extensional flow properties were included in viscosity model[68]. Yet both are usually omitted in the simulation, most probably because of the lack of experimental data for molding materials.

4.3   Rheology in extrusion

Extrusion is a continuous process, where the boundary conditions are given by the geometry of the die and the calibrator. The polymer resin is conveyed, homogenized and compressed by a rotating screw, and the form is given by the die through which the melt

flows. Conveying in the screw takes place by drag flow, and the die causes an opposing pressure flow that resists the drag flow. Flow rate in the screw conveying zone is determined by the resin viscosity, screw rotation speed and screw and channel geometry.

The output of a conventional single-screw extruder can be determined by the operating diagram (Figure 19), which takes into account the characteristics of the used screw and die. In this highly simplified approach the flow is assumed to be Newtonian and isothermal. The operating point of the screw-die combination is set by the intersection of the characteristic curves of screw the die. The maximum flow rate, drag flow rate Q_d, is achieved only when the resisting back pressure P of the die equals zero (open discharge, no die). The flow resistance of the die depends on its geometry.
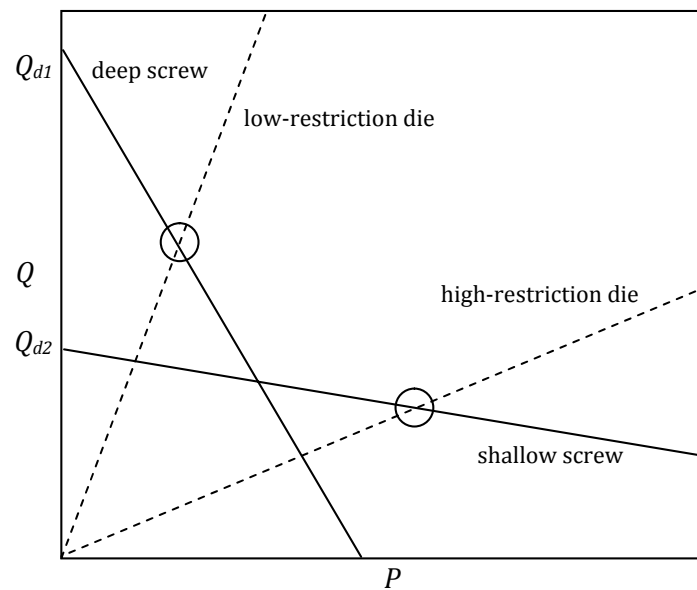
Figure 19. Example of an operating diagram for two different screw and die geometries. The process conditions for each screw–die combination is determined by the intersection of their characteristic curves.

In reality, the flow is non-Newtonian and non-isothermal: shear thinning lowers the viscosity, and a great part of the work is dissipated as heat, which is not fully conducted away through the barrel and screw, but decreases the melt viscosity further. In addition, different zones of the extruder screw have their effect on the net flow. In case of non-Newtonian fluid the characteristic curve of the die takes a non-linear shape, and the characteristic screw curves also vary according to the Power-law index of the melt, being linear only when $n=1$, that is, the fluid is Newtonian (Figure 20)[1].

Figure 20. Normalised characteristic screw and die curves in case of non-Newtonian fluids

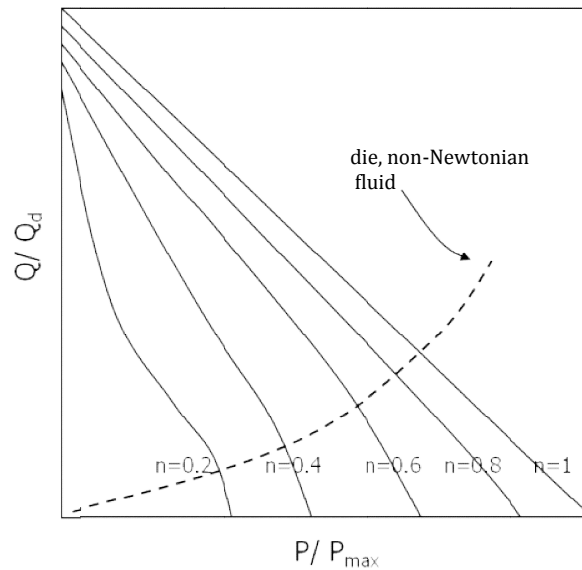Simplified analysis assumes the flow rate to depend only on the screw rotation speed. As can be seen in Figure 19, with a deep screw the best output is achieved using a low restriction die, whereas a shallow screw gives maximum output with a higher-restriction die. In real cases, however, multiple possible operating points, that is, combinations of temperature, pressure and flow rate, can be found[1].

4.3.1 *Effect of viscoelasticity on die swell and extrusion instabilities*

The viscoelastic nature of the polymer melts is the origin of many peculiar phenomena faced in polymer processing and various polymer processing difficulties have been associated with extensional flow properties[13]. Viscoelasticity manifests itself in extrusion as die swell: long, entangled and coiled molecules are forced to partly orientate along the flow when the stream converges at the entrance to a narrow die. However, the "memory effect" of the viscoelastic materials makes them to gravitate back to the original, un-oriented state at the die exit. This is seen as an expanded cross-section of the extrudate, die swell (Figure 21). The effect is more pronounced for polymers with high degree of branching and high molecular weight. The degree of swelling is further set by die and resin temperature and the L/D ratio of the die: In a long die the molecules orient more with the flow, relaxate and "forget" part of their original coiled state, therefore swelling less at the die exit. In a flow through a short die a smaller part of the original coiling is lost and the die swell at the exit is greater. Swell in the circular dies is the simplest case, because the extrudate shape is not distorted. In case of non-circular profiles the shape also changes at the exit[1]. Die swell measurements can be used to qualitative estimations of elasticity.
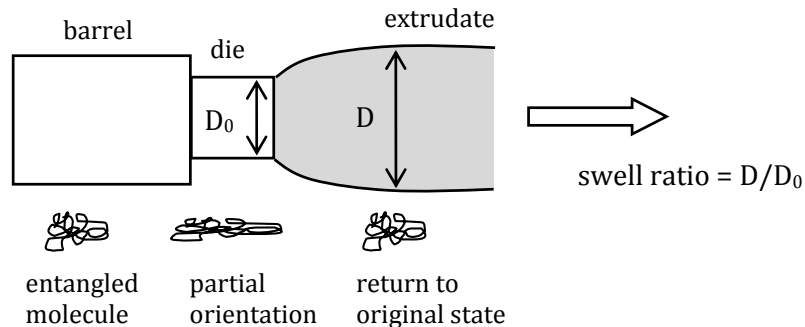
Figure 21. Representation of die swell

Melt flow instability occurs when a critical shear stress τ_c, is exceeded. Therefore the maximum rate in extrusion process is limited by the onset of flow instability. This causes extrudate distortion, varying from minor loss of surface gloss to a rough, spiral-like melt fracture. Melt fracture types can be divided into volume distortions and surface distortions according to the depth of occurrence within the extruded polymer strand. Surface distortions, often described according to their appearance as shark skin or screw thread, originate at the die exit, whereas volume distortions, which show as a helical, wavy or chaotic extrudate, originate at the die entry[16].

Reasons of melt fracture are various: Die geometry and material, processing conditions (temperature, flow rate), as well as the chemical nature and molecular architecture of the polymer all have an influence on its occurrence. Nevertheless, its mechanisms are still not fully understood. Several theories on both macroscopic and microscopic level have been presented. In most of them, extensional rheology and elasticity plays a significant role. According to one theory, the surface layer of an extrudate accelerates at die exit, leading to high level of surface stretching, while the extrudate core decelerates (Figure 22). High elasticity retards the stress growth at the surface, and therefore more elastic, highly branched and high M_w polymers tolerate higher strain rates without melt fracture. Another theory suggests that the fracture of the surface layer is caused by melt sticking and slipping at the die exit: The core flows constantly while the surface grows a ridge of melt to the die exit, which then detaches along the flow, and a new melt ridge starts to form causing an alternating stick-slip phenomenon[16].
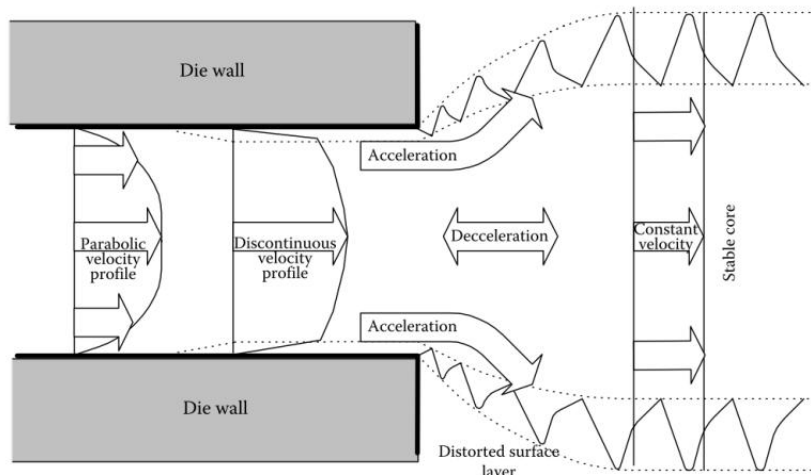

Figure 22. Representation of surface distortions due to acceleration of the extrudate outer layer[16]

4.4 Rheology in extensional flow dominated processes

Extensional flow dominates especially in processes where free flow surfaces exist; the polymer is stretched or oriented in uniaxial, biaxial, or planar manner. Many secondary shaping methods, such as fiber spinning (uniaxial extension), film blowing (biaxial and planar extension) and blow molding (uniaxial, biaxial and planar extension) are examples of extensional flow processes. In order to correctly model the polymer flow in such processes, rheological characterization in extension instead of (or in addition to) shear is essential. Extensional viscosity is a very sensitive indicator of changes in molecular architecture, such as long-chain branching, which has a great impact on the performance of polymers in processes involving a high degree of stretching. Shear viscosity, on the other hand, does not readily reveal such properties: Two polymers with completely different extensional behaviors (e.g. extension thickening – extension thinning) can have virtually the same zero-shear viscosity and flow curve, which does not tell anything about their different stretchability[13].

4.4.1 Fiber spinning

Spinning of fibers from polymer melt involves strong axial orientation in uniaxial flow: The polymer melt is extruded through a spinneret die and drawn and spooled on a roll at a pre-determined take-up speed. The take-up speed is much higher than the extrusion speed, which leads to a high degree of uniaxial stretching. The process is highly non-isothermal as the thread is cooled during drawing before the take-up. The relationship of take-up speed to the extrusion speed is called the draw ratio, and in industrial processes it is generally about 5:1[76]. When the draw ratio exceeds a critical limit, instable flow, draw resonance, occurs. Polymers preferred for melt spinning have a low level of chain branching at a high degree of polymerization[77]. However, sensitivity to draw resonance is higher for linear than for long-chain branched, strain hardening (and extension thickening) polymers[78,79,80]. The Rheotens test mentioned in Chapter 3.6 is a good representation of fiber spinning and useful for evaluating the performance of polymers in such manufacturing processes[47].

4.4.2 Blow molding

Blow molding, a common method for manufacturing, for example, beverage bottles, can be divided into two categories according to the method for forming the preform of the moldable article. In injection blow molding (also: stretch blow molding) the preform is first injection molded, cooled down, transferred to a blowing station, where it is again heated to the required stretching temperature and formed into a hollow object by biaxial stretching using pressurized air (and a stretch rod).

In extrusion blow molding the final forming takes place instantaneously after extrusion of the tube-like parison; an automated mold pinches the parison end to form the bottom of the bottle, inflated by air blown from the upper end of the mold which also forms the neck of the bottle.

Both of these manufacturing processes involve shear (extrusion/ injection molding of the preform) and extensional deformation (blowing phase). Especially in extrusion blow molding the flow is a complex combination of different factors: swelling at the die exit due to the memory effect of the macromolecular compound, uniaxial extensional flow due to vertical gravitational sagging of the extruded tube before it is taken by the blowing mold, and finally mixture of planar and biaxial stretching due to the blowing pressure. Sag and die swell of the preform occur simultaneously after extrusion and are

counteracting regarding the parison length, which makes the estimation of the parison behavior rheologically challenging[1] (Figure 23).
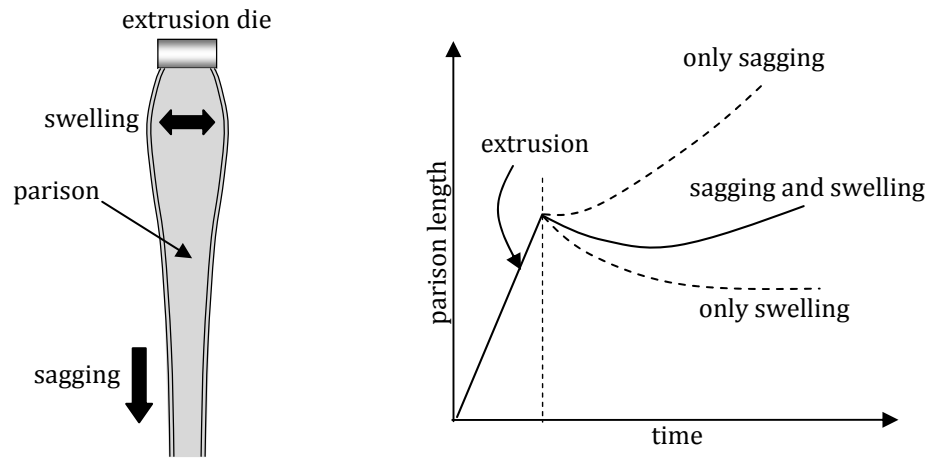

Figure 23. The effect of sagging and die swell in the extrusion blow molding parison

4.4.3   Film blowing

Blown film manufacturing involves vertical extrusion through an annular die, where air stream in the middle is applied to expand the extruded tube through planar and biaxial extension into a bubble of thin tubular film. The film bubble is cooled by air streams while drawn vertically and finally collapsed and wound to a spool located above the die. Before exiting the die, the polymer experiences shear flow, but during the stretching phase the flow is essentially shear free. The process is further complicated by its highly non-isothermal nature, whose understanding requires knowledge of the behavior of solid polymer near the transition temperatures[1,81]. The process requires a fine balance between the temperature, extrusion rate, drawing rate and blown air pressure in order to achieve high quality film with equal thickness throughout, while maintaining the film tube diameter constant. One significant factor affecting the bubble stability is the extensional flow behavior of the melt. Long-chain branching and high M_w fractions increase the strain hardening and extension-thickening of polymers, and polymers with these properties, e.g. LDPE, exhibit better bubble stability[78,82] and are thus preferred in the film blowing process.

5 SUMMARY OF EXPERIMENTAL WORK AND RESULTS

In this part a brief summary of the work done in each publication and the central results and conclusions as well as suggestions for further research are given. The first subchapter gives a brief summary of all tested materials and test methods.

5.1 Test materials and experimental settings

Commercial thermoplastic grades designed mainly for extrusion or injection molding were used in all the studies (Table 1).

Table 1. Polymer grades used in the experiments discussed in publications. Properties are provided by the suppliers.

Supplier	Polymer	Trade name	Density [kg/m³]	MFR [g/10min] / MVR [cm³/10min]	Publication
(Lyondell) Basell	LDPE	Lupolen 1840H	919	1.5 g/10 min (190°C, 2.16kg)	II, III
		Lupolen 3020D	926	0.30 g/10 min (190, 2.16)	IV, V
	PP	Moplen EP340K	900	4.0 g/10 min (190, 2.16)	III
		Moplen HP501L	900	6.0 g/10 min (230, 2.16)	VI
		Moplen HP501H	900	2.1 g/10 min (230, 2.16)	VI
BASF	PS	Polystyrol 143E	1040	10 cm³/10 min (200, 5.0)	I, II, III, VI
		Polystyrol 158K	1050	3.0 cm³/10 min (200, 5.0)	VI
	ABS	Terluran GP-22	1040	19 cm³/10 min (220, 10)	III
GE Plastics	PC	Lexan HF1110R	1200	26 cm³/10 min (300, 1.2)	I, III
Degussa	PMMA	Plexiglas 6N	1190	12 cm³/10 min (230, 3.8)	I

ABS, PC, and PMMA were always dried in a vacuum oven or desiccator according to the suppliers' recommendations before rheological characterization.

Anton Paar MCR301 rotational rheometer with CTD600 convection oven was used for low-shear rate rheological characterization: For dynamic oscillation tests a 25 mm parallel-plate geometry, and for steady-shear tests a 25mm cone-plate geometry with a 2° cone angle was used. Uniaxial extensional experiments (Publications IV and V) were done with SER "1st generation" extensional fixture connected to Anton Paar MRC301 with CTD450 convection oven (device located at Berlin Institute of Technology). All the experiments by rotational rheometer were carried out under a protective nitrogen atmosphere.

Capillary rheometry experiments were all done using Göttfert Reograph 6000 three-bore capillary rheometer. Depending on the case, circular dies with L/D of 5, 10, 20, and 30 were used, and the entrance pressure drop was measured using an orifice die with a conically expanding outlet, a standard design provided by Göttfert. Viscosity measurements at elevated pressure were produced using a counter-pressure chamber, also a standard device by Göttfert.

Viscosity measurements with an injection molding machine (Publication VI) were done using the all-electric injection molding machine Fanuc Roboshot α-30C with a tailor-made slit die with exchangeable inserts for slit heights 0.75, 1, and 1.5 mm. Pressure data was collected with the Agilent 34970A data acquisition unit.

Samples for rotational rheometer were prepared from the resins by hot-pressing the granulates by a heated press into a thin plaque, from which round discs with 25 mm diameter were punched or cut out. For extensional experiments the resin was first homogenized by a single screw extruder and after that pressed into a sheet between PTFE foil-covered aluminum plates in a hot press. The sheets were cooled down slowly at room temperature between the press plates and under a heavy weight to avoid warpage and to eliminate the possible effects of shearing, to which the melt is subjected in the extruder. After cooling, rectangular strips were cut out of the pressed sheet.

5.2 Viscosity at low shear rates and temperatures (Publication I)

The accuracy of the simulation of injection molding process is dependent on the ability of the viscosity model to describe the behavior at the shear rates, temperatures and pressures involved in the process. Commercial simulation software use GNF equations to predict the melt viscosity. Commonly the measurements are carried out at relatively high temperature, corresponding to the polymer's processing temperature. Injection molding, however, is a highly non-isothermal process including phases of high shear and high temperature, such as the filling phase, and low shear and low temperature, such as the packing phase. The purpose was to study the applicability of a GNF equation in modeling the viscosity of polymer melts in the latter cases.

The Carreau-Yasuda model is a five-parameter GNF model and was used here with the WLF equation for temperature dependence to characterize the flow behavior at low-temperature, low-shear flow region for three amorphous polymers: PS, PMMA, and PC. First, a temperature sweep test in dynamic mode was performed to get an indication of the solidification point and thus the lower temperature limit for frequency sweep tests. The lowest measurement temperatures that could be realized without exceeding the torque limit of the device or detachment of the sample off the measuring plates was around 20 °C above the glass-transition temperature of each polymer. The experimental viscosity data was obtained from the dynamic oscillatory measurements using the Cox-Merz approach to relate the complex viscosity vs. angular frequency to viscosity vs. shear rate. The Carreau-Yasuda-WLF fitting was applied on the experimental data, and generally a good fit could be achieved. However, at lowest temperatures and highest angular frequencies a leveling-off of the viscosity curves towards the apparent 2nd Newtonian plateau could be observed for the studied materials, and the used viscosity model as such was not able to model this trend. Whether this really indicates the actual 2nd Newtonian plateau, remains rather uncertain on the basis of present data: the measurements were made in the dynamic mode and the Cox-Merz rule was applied. However, the Cox-Merz empirical relation was originally applied at temperatures way above the glass-transition[6], and – to the authors' knowledge – has not been validated close to the polymer's solidification temperature. Results showing an apparent 2nd Newtonian plateau for various polymers have been achieved at high shear rate, usually around 10^6 s^{-1}, with specially designed capillary rheometers and dies coupled to the nozzle of an injection molding machine[31,32,33,83,84].

Considering the relevance for injection molding process, the important regions in viscosity modeling are the low temperature – low shear and high temperature – high shear flows, thus the fact that the apparent 2nd Newtonian plateau cannot be predicted by the viscosity models commonly used by flow simulation software is not crucial for the correct process parameter estimations. The crystallization phenomenon makes the solidification behavior of semi-crystalline polymers dependent on several variables[9,85,86], and is therefore more complex than that of amorphous polymers. Crystallization kinetics depend on the time, temperature, cooling rate, and deformation rate and type: viscosity measurements at low shear rate/ angular frequency take a long time, during which the crystallization is possible in principle at any temperature below the polymer's melting temperature, but the crystallization rate and degree depend on the test conditions. A further study of the flow properties at low-shear, low-temperature region for semi-crystalline polymers would provide more information about the applicability of viscosity fit functions for them.

Appendix 2 presents corrected results for PS at 170, 190 and 230 °C, at which the measured viscosity in the originally published paper was below the expected level.

5.3 Determining the entrance pressure drop in capillary rheometry (Publication II)

One of the main assumptions in capillary rheometry is that the flow is fully developed. However, in order to achieve true shear viscosity by a capillary rheometer, the extra pressure drop caused by the acceleration and stretching of the melt at the entrance of the capillary must be taken into account in the calculation procedure. This is usually taken into account by applying the Bagley correction, as briefly explained in Chapter 3.2. Another option for correction of the entrance pressure drop, a direct measurement of the entrance pressure drop with an orifice die, was studied here. Direct measurement of entrance pressure drop simplifies the procedure and saves time, but apparently the geometry of the die affects the measurement accuracy: the geometry used here has a conical, gradually expanding outlet area, and for some materials sticking to the outlet wall causes a higher entrance pressure drop than what could be determined by the conventional Bagley correction. The orifice die used here has a true length of 0.2 mm. In order to ensure sufficient rigidity of the die, a conical expansion area at the outlet is necessary for such a short die with a flat, 180° inlet.

In this study PS and LDPE were used as test materials. Capillary rheometer measurements were performed using dies with the L/D ratio 0 (orifice die), 5, 10, 20, and 30. The entrance pressure drop measured with the orifice die (Δp_{e0}) was compared to the one extrapolated from Bagley plots (Δp_{eB}), which were constructed at each measured shear rate from the pressure recordings measured with the four longer capillaries. However, for PS the results with die L/D=30 were excluded, as they did not fall on a straight line with the pressure recordings with shorter dies. The upwards deviation of the L/D=30 in Bagley plots is explained by the pressure effect on viscosity: In a long die the pressure can get high enough to increase the viscosity of the melt. The significance of this is dependent on the general pressure dependence of the viscosity, which is known to be greater for PS than for LDPE.

The extra pressure drop evolving within the outlet area was numerically modeled (Δp_{Calc}) using the Comsol Multiphysics software. Generalized Newtonian fluid with isothermal creeping flow was assumed, with axial symmetry and the no-slip condition at the outlet wall. Shear thinning behavior was described by the Carreau-Yasuda model (Eq. 29). The computing situation models the case where the outlet region is full of melt, which means that the sticking of the melt is at its maximum. Thus the difference of the entrance pressure drops Δp_{e0}-Δp_{eB}, should approach Δp_{Calc} when the sticking increases.

For both materials the measurements with the orifice die gave a higher entrance pressure drop than the Bagley correction. The difference between Δp_{e0}-Δp_{eB} was greater for PS, which suggests that it sticks more to the outlet wall than LDPE. Also the comparison of Δp_{e0}-Δp_{eB} to Δp_{Calc} confirmed this, although the differences in the sticking behavior cannot really be observed visually during the measurement. Another factor for the smaller difference in results for LDPE might be its higher relative extensional viscosity: this manifests itself as stronger corner vortex formation in the contraction flow, and therefore higher entrance pressure drop, which in turn leads to smaller Δp_{e0}-Δp_{eB}. The outlet area increased the total entrance pressure drop with increasing shear rate by a factor from 1.3 to 1.5 for LDPE and by 1.4 to 2.1 for PS. Factor of 1.5 was suggested here to correct the error caused by the sticking, so that the corrected entrance pressure drop Δp_e= Δp_{eB}/1.5. The applicability of this correction factor to other materials has not been proved.

Sometimes the extraction of the entrance pressure drop is bypassed using only one long capillary die without any correction. In a long capillary the relative portion of entrance pressure drop is indeed small, but at the same time viscous heating and pressure dependence of viscosity may corrupt the results. Here, the use of orifice die data for the entrance pressure drop correction gave results closer to the Bagley corrected ones than the use of a die with L/D=30 alone. For further use of the direct measurement method, the best solution would be finding an ideal orifice die geometry that allows free exit of the extruded melt.

5.4 Viscosity at elevated pressures (Publication III)

When polymer melts are subjected to a high pressure, their viscosity is affected by the pressure, increasing with increasing hydrostatic pressure. The pressure dependence of viscosity of polymer melts becomes important when the pressure in the manufacturing process gets high enough. Generally, such a situation occurs in injection molding, and more specifically in the mold filling and packing phase. Compressibility and the dependence of viscosity on the pressure for a polymer melt is largely dependent on its structure; in general amorphous polymers with large pendant groups, ring structures and double bonds in the backbone possess more free volume and thus are able to compress to a higher degree.

Viscosity at elevated pressure was measured for five commercial thermoplastic polymers; PC, ABS, PS, PP and LDPE, to find out the significance of the pressure dependence of viscosity for each. The experiments were carried out by a capillary rheometer with an additionally mounted pressure chamber with a maximum mean operating pressure of 120 MPa. For each polymer, measurements were done at a typical processing temperature at shear rates 50, 100, 200, and 500 (for PC also 1000 s^{-1}), so that during each test the shear rate was held constant and the mean pressure was gradually increased by constricting the downstream flow in the chamber. An orifice die and a die with *L/D* = 10 were used, and the correction for the entrance pressure drop was done according to the procedure suggested in Publication II. Pressure was recorded upstream and downstream of the capillary by two transducers, and the total pressure drop across the die is the difference between their readings. In order to get low-shear rate data inaccessible by a capillary rheometer, a rotational rheometer with a cone-plate geometry was used at ambient pressure.

As the experimental setting does not allow exact adjustment of the upstream pressure, the data points achieved with both capillaries were fitted on a quadratic curve in order to be able to extract the entrance pressure drop (measured with the orifice die) from the pressure drop of the die with *L/D*=10. Data handling also included a correction for the non-parabolic velocity profile in the die. For this the Schümmer approximation[24,25] was used: the shear rates were multiplied by 0.83. The pressure

coefficient that describes the pressure dependence of viscosity was obtained by time-pressure superposition of the data measured at different pressures. The data are compiled to a master curve at ambient pressure (p=0.1 MPa) by shifting them with a pressure shift factor.

The Carreau-Yasuda equation was fitted on the high-pressure data for modeling the viscosity, and the cone-plate data was included in the fit for better description of the low-shear rate region. However, for ABS no leveling-off towards the Newtonian plateau could be observed, and instead of the Carreau-Yasuda equation, power-law fitting was used and the low-shear data was omitted from the fit. For PC, the Newtonian plateau was reached already in capillary rheometer measurements, and no additional cone-plate data was necessary.

The order of the pressure coefficients was PS > PC > ABS > PP > LDPE. As expected, the amorphous polymers have a stronger pressure dependence of viscosity than the semi-crystalline ones. Regarding the relationship of pressure dependence to the complexity of the molecular structure, one would think PC would have a stronger pressure dependence of viscosity than PS. However, considering the temperature dependence of pressure coefficient the order makes sense, as the test temperature of PS was much closer to its T_g than the test temperature of PC. A theoretical perusal of pressure dependence of viscosity in injection molding was made on the basis of the pressure coefficient achieved for PS. Including the pressure shift factor in the calculation at a hypothesized pressure in mold filling situation, p=200 MPa, increased the viscosity at high shear rates multifold compared to the situation where no pressure dependence of viscosity is taken into account.

5.5 Measurement of uniaxial extensional viscosity by SER (Publication IV)

SER is a relatively simple device for characterizing the extensional flow properties of polymer melts. However, certain limitations must be taken into account and some corrections need to be done in order to get accurate, reliable results. The basic procedure in evaluating the measured extensional viscosity data should always include checking against the linear viscoelastic limit as the first step of result validation: for uniaxial extension, in the slow-flow region of transient start-up flow, that is, low Hencky strain rates, the transient extensional viscosity should be related to the start-up shear viscosity η_s^+ as illustrated in Figure 7 and Eq. 23, so that in uniaxial extension the LVE $\mu_0(t) = 3\eta_s^+(t, \dot{\gamma}_s \to 0)$. In many rheology laboratories the LVE for extensional start-up curves is found to lie above this, and a simple shift of data downwards is performed to "correct" the results, without thinking of the reasons for this discrepancy. The steady-state flow indicated by the leveling of the start-up extensional viscosity towards a constant value can most often not be achieved by SER due to instability and rupture of the sample, and maximum values, rather than steady state values, should be reported.

In this study the extensional viscosity of LDPE at three different temperatures, 170, 180, and 190 °C, was measured by SER using different testing and calculation procedures. The accuracy and correctness issues related to experiments and calculations were discussed in detail. The results were compared with the ones obtained earlier by RME and MTR[87] and the comparability with theoretical approach was studied through application of the Molecular Stress Function (MSF) model[88,89].

The best results were achieved when the measurements were performed using a long pre-tempering time of the device, mounting the temperature sensor tight next to the SER frame, and fixing the sample without clamps. The two first factors are related to the temperature control of the device and applied in order to ensure proper heating of the SER device and uniform temperature distribution throughout the sample. The third factor apparently has an effect on the deformation at the sample strip ends: attaching

the sample with clips can cause a partially planar deformation field, so that the assumption for uniaxial extensional flow does not fully hold. In addition to these measures, the experimental data were corrected by taking into account the changes of the sample dimensions because of thermal expansion and pre-stretching: The calculation takes into account the density of the sample at solid state, but heating the sample causes expansion that has to be corrected by using the melt density at test temperature. Pre-stretching is needed in order to avoid sagging of the sample during the heating phase, as discussed in Extensional Flows (Chapter 2.3). Correct sample dimensions at the beginning of the test are thus achieved by taking into account the decrease of the sample width and thickness caused by drum rotation (initial deflection angle φ_0) in the pre-stretching phase.

After the experimental and correction procedures summarized above the measured strain hardening function of LDPE was well in accordance with the RME and MTR measurements, although the maximum values achieved in transient SER tests were lower. The MSF model was able to describe the strain hardening behavior at all three temperatures by the same non-linear parameters. The work conducted for this paper was carried out in cooperation with Anton Paar GmbH rheometer manufacturer, and the outcome led to improvements of the software module used when measuring the extensional viscosity by SER: in the current version it is possible to feed the melt density of the sample as an input parameter, and it is taken into account in the calculation. The experiments were performed using only one material, a commercial LDPE. In order to prove and develop the technique further, a broader study using polymers with different properties is suggested.

5.6 Comparison of uniaxial extension and contraction flow analysis (Publication V)

The maximum values from the transient extensional viscosity tests for LDPE by SER, reported in Paper IV, were compared to the results obtained by Cogswell approximation method. In addition, the MSF model was applied to describe the experimentally achieved $\eta_e(\dot{\varepsilon}_H)$. For Cogswell analysis, capillary measurements were performed by Göttfert Rheograph 6000 capillary rheometer using a round-hole die with a diameter of 1 mm and L/D of 20. In addition, an orifice die was used to measure the entrance pressure drop Δp_e directly according to the procedure presented in Publication II. Both dies have an abrupt contraction at the entrance, i.e. the entrance angle is 180°. The measured set covered the shear rates 10, 20, 40, 100, 200, 400, 1000 s^{-1}.

The Cogswell analysis[19] is based on the assumption that shear and extensional components of an additional pressure drop at flow contraction can be separated: When the polymer fluid flows through a sudden contraction, the center of the flow region is funnel-shaped, whereas, due to the elastic effects, circulating flow vortices are formed at the corners. These vortices dissipate energy, causing an extra pressure drop at the entrance region of the contraction. The contribution of the extensional effects can be calculated according to Cogswell by deriving it from the entrance pressure drop, Δp_e which is assumed to be the sum of pressure drops caused by shear and elongational deformation.

When extensional viscosity obtained by two different methods is compared, it is critical that the total strain, rather than the strain rate, is equal in both. Indeed, the average maximum strain in the SER tests, $\langle \varepsilon_{max} \rangle \approx 3$, agrees with the average strain at the capillary flow contraction with the barrel/ die cross-sectional area $A_b{:}A_d = 144$. A relatively good correlation between these two methods was found for the LDPE test material. This suggests that using the Cogswell analysis may be sufficient when evaluating extensional properties for needs of process modeling, such as injection molding simulation, and no accurate information of the polymer structure-behavior

relationship is sought. The MSF theory predicted higher steady-state extensional viscosity values, which is readily explained by the fact that the strain level corresponding to the steady state was not reached in the experiments. Reapplication of the MSF model at $\varepsilon = 3$ resulted in a remarkable agreement with the experimental data.

As an extension to the present work, the compatibility of the Cogswell method and uniaxial extensional measurements should be proved with other type of polymers. Moreover, studying extensional viscosity achieved by different experimental methods and by theoretical predictions would be an interesting topic for future research, combined with the study of extensional flow in the injection mold cavity. Molecular modeling, such as MSF theory, could offer an interesting possibility to theoretically achieve data needed for processing applications, when only a limited number of experimental results are available.

5.7 Viscosity measurements of polymer melts by an adjustable slit die and injection molding machine (Publication VI)

Shear viscosities of two grades of PP and two grades of PS were measured with a slit die connected to an injection molding machine. The slit die was tailor-made and designed to fit both extruders and injection molding machines. The die has a modular construction, designed to allow a variation of the slit height by exchanging the slit insert. The height can be set to 0.75, 1.0 or 1.5 mm, all having the same width, 15 mm. The benefits of this flexibility become obvious when various materials with highly different flow properties are characterized. Another point is that by performing measurements using all the slit heights, one can detect possible wall slip as a discrepancy in the flow curves or viscosity curves achieved with different slit sizes. To allow the practical mounting of temperature sensor in the middle of the die, this design has only two bores for pressure transducers.

The die was fixed to the stationary mounting plate of Fanuc Roboshot α-30C all-electric injection molding machine. Measurements were carried out at 200 and 230 °C at pre-set injection speeds so that the shear rate varied approximately from 400 to 20 000 s^{-1}. Slit pressure was measured at two points with a distance of 55 mm with Dynisco pressure transducers. For all the polymer grades studied here, an excellent agreement of viscosity measured by the injection molding machine with a slit die and a conventional off-line rheometer was achieved. Slit die measurements with an injection molding machine provide an easy-operation, fast and sufficiently precise option for measuring shear viscosity of polymer melts at relatively high shear rates typical of polymer melt processing. Because of the screw plasticizing, the thermo-mechanical history of the melt is similar to the processing conditions. Modular design with detachable slit inserts facilitates proper cleaning of the die, thus eliminating one of the major downsides associated with slit die constructions.

In order to extend the usability of the initial slit die design tested here, adding a constriction valve downstream the flow has been considered: this way the back-pressure of the die could be regulated, enabling measurement of viscosity at elevated pressures. The all-electric injection molding machine used in these tests proved to be very precise: good agreement with off-line rheometry indicates that exact calculation of the flow rate from the injection speed and screw diameter is possible – which is an essential requirement for a rheological measurement device. However, the machine used in the current study has a relatively small capacity, and in order to study viscosity at extremely high shear rates and/or elevated pressures, a machine with a higher shot volume and injection pressure capacity should be used.

6   CONCLUDING REMARKS

This work aimed at extensive rheological characterization of thermoplastic polymers, necessary for understanding the flow behavior of the melt in polymer processing, especially in injection molding. Certain issues related to the accuracy and correctness of experimental and analytical procedures were also considered. Thus the purpose of this work is not only enhancing the knowledge of the significance of polymer melt rheology for improving the accuracy of injection molding simulation, but also pointing out some of the important issues related to correct measurement procedures useful in polymer processing and research in general.

Publication I on measuring and modeling viscosity at low temperature and shear rates, reports a situation faced in the packing phase of injection molding. For the flow phases relevant in injection molding – high temperature and high shear rate, as in filling, or low shear rate and low temperature, as in packing – a GNF model, such as the Carreau-Yasuda equation, was able to describe the viscosity function accurately.

Publication III reported the pressure dependence of viscosity for several polymers. The pressure dependence of viscosity is highly dependent on molecular structure: A complex structure possesses more free volume, and is thus more strongly affected by compression, which causes the polymer chains to inhibit each others' movements and thus increase viscosity. At lower temperatures, close to the T_g, the effect of pressure on viscosity is more pronounced. This has an effect on the simulation accuracy when the polymer's pressure dependence factor is large enough and the pressure level in the process gets relatively high.

Some factors affecting the measurement quality related to capillary rheometry and uniaxial extension by counter-rotating drum device were considered. Publication II deals with the correction of entrance pressure drop in capillary rheometry: Orifice die is a good alternative for evaluating the entrance pressure drop, but the conical outlet geometry of the commercial design used here requires a correction for the additional pressure drop caused by the adhesion of the melt to the outlet wall.

Publication IV examined the experimental and analytical practice and errors in uniaxial extensional experiments by SER. It was shown that by taking into account the changes in sample geometry due to thermal expansion and pre-stretching, more exact results can be achieved. The author was in close cooperation with the rheometer manufacturer Anton Paar GmbH when the measurement protocol and calculation routine were evaluated. As one important outcome of this study, the Anton Paar software module used to operate SER has been improved by adding an option of taking into account the geometrical error related to the thermal expansion.

A combination of two methods for determining extensional viscosity at broad-extension rate range – considering injection molding simulation as a possible application – was studied in Publication V. Extensional viscosity could be achieved over a wide range of extension rates with relatively good accuracy by measuring it using SER and by evaluating from contraction flow analysis on capillary rheometry data. Moreover, the MSF model was able to predict the extensional behavior in case where scarce experimental data is available.

Publication VI studied an alternative equipment for measuring rheological properties: A slit-die connected to injection molding machine produced viscosity results very well comparable to the ones achieved by capillary and rotational rheometer. It was proposed as an attractive option as a low-cost, easy-operation rheometer for industrial purposes. Moreover, with the current design it is possible to study wall slip and the effects of pre-shearing on the viscosity, and so to characterize the polymer melts under true processing conditions. With modifications the slit geometry could also be used to study the effect of pressure on viscosity.

To summarize the achievements of this work briefly, some particular points can be named: As an important outcome of this study, the knowledge about the sensitivity of the measured rheological parameters to the test device design and to the realization of the experimental procedure – such as the appropriate orifice die geometry in capillary rheometry, or the determination of the uniaxial extensional viscosity by SER – has increased. To the author's knowledge, the errors related to the experiments with SER were for the first time examined and reported in this extent. The importance of careful sample preparation, planning and realization of experiments was also emphasized. Furthermore, general knowledge on the impact of viscoelastic phenomena which can have important effects in polymer processing, has increased. The functionality of a low-cost tailor-made rheological device was demonstrated, and this kind of easy-operation "rheometer" was proposed as an attractive alternative for industrial use and for measuring polymer melt viscosity under true processing conditions. Using the MSF theory to complement and validate experimental methods was an educative case and a good example of the potential usefulness of a theoretical approach in practice. As a suggestion for future studies and validation of the results achieved within this work, the discussed topics should be extended to embody a bigger set of experimental data for various types of polymers, such as fiber-filled polymers and thermoplastic elastomers.

7   REFERENCES

1 Dealy JM, Wissbrun, KF. Melt rheology and its role in plastics processing – Theory and applications. Dordrecht: Kluwer Academic Publishers; 1999. 665 p.

2 Dealy JM, Larson RG. Structure and rheology of molten polymers – From structure to flow behavior and back again. Munich: Carl Hanser Verlag; 2006. 516 p.

3 Morrison, FA. Understanding rheology. New York: Oxford University Press; 2001. 545 p.

4 Kulicke WM, Porter RS. Irregularities in steady state flow for non-Newtonian fluids between cone and plate. Journal of Applied Polymer Science 23, 1979, 953-965.

5 Larson RG. Instabilities in viscoelastic flows. Rheologica Acta 31, 1992, 213-263.

6 Cox WP, Merz EH. Correlation of dynamic and steady flow viscosities. Journal of Polymer Engineering and Science 28, 1958, 619-621.

7 Ferry JD. Viscoelastic properties of polymers. 2 Ed., New York: John Wiley & Sons, Inc.; 1970. 671 p.

8 Williams ML, Landel RF, Ferry JD. The temperature dependence of relaxation mechanisms in amorphous polymers and other glass-forming liquids. Journal of the American Chemical Society 77, 1955, 3701-3706.

9 Filipe S, Knogler B, Buchmann K, Obadal M. Shear and extensional flows as drivers for the crystallization of isotactic polypropylene – When rheology, microscopy and thermal analysis must meet. Journal of Thermal Analysis and Calorimetry 98, 2009, 667-674.

10 Dealy J, Plazek D. Time-Temperature Superposition - A Users Guide. Rheology Bulletin 78(2), 2009, 16-31.

11 Hieber CA in: Injection and Compression Molding Fundamentals. ed. Isayev AI, ch.1, New York: Marcel Dekker; 1987.

12 Cogswell FN. The influence of pressure on the viscosity of polymer melts. Plastics & Polymers, 41, 1973, 39-43.

13 Baird DG. The role of extensional rheology in polymer processing. Korea-Australia Rheology Journal 11(4), 1999, 305-311.

14 Hieber CA, Chiang HH. Shear-rate-dependence modeling of polymer melt viscosity. Polymer Engineering and Science, 32(14), 1992, 931-938.

15 Macosko CW. Rheology: Principles, measurements and applications. New York: Wiley-VHC, Inc.; 1994. 581 p.

16 Koopmans R, den Dolder J, Molenaar J. Polymer melt fracture. Boca Raton, FL: Taylor and Francis Group LLC; 2011. 311 p.

17 Bagley EB. End corrections in the capillary flow of polyethylene. Journal of Applied Physics 28, 1957, 624-627.

18 Mooney M. Explicit formulas for slip and fluidity. Journal of Rheology 2, 1931, 210-222.

[19] Cogswell FN. Converging flow of polymer melts in extrusion dies. Polymer Engineering and Science 12, 1972, 64-73.

[20] Binding DM. An approximate analysis for contraction and converging flows. Journal of Non-Newtonian Fluid Mechanics 27, 1988, 173-189.

[21] Nelson B, Capillary Rheometry in: Handbook of Plastics Analysis. Ed. Lobo H, Bonilla JV. New York: Marcel Dekker Inc.; 2003.

[22] Laun HM. Polymer melt rheology with a slit die. Rheologica Acta 22, 1983, 171-185.

[23] Laun HM. Pressure dependent viscosity and dissipative heating in capillary rheometry of polymer melts. Rheologica Acta 42, 2003, 295-308.

[24] Chmiel H, Schümmer P. Eine neue Methode zur Auswertung von Rohrrheometer-Daten. Chemie Ingenieur Technik 1971, 43(23), 1257-1259.

[25] Schümmer P, Worthoff RH. An elementary method for the evaluation of a flow curve. Chemical Engineering Science 33, 1978, 759-763.

[26] Giesekus H, Langer G. Die Bestimmung der wahren Fließkurven nicht-Newtonischen Flüssigkeiten und plastischen Stoffe mit der Methode der repräsentativen Viskosität. Rheologica Acta, 16, 1977, 1-22.

[27] Padmanabhan M, Bhattacharya M. In-line measurement of rheological properties of polymer melts. Rheologica Acta 33, 1994, 71-87.

[28] Bariani PF, Salvador M, Lucchetta G. Development of a test method for the rheological characterization of polymers under the injection molding process conditions. Journal of Materials Processing Technology 191, 2007, 119-122.

[29] Qin X, Thompson MR, Hrymak A. Rheology studies of polyethylene/ chemical blowing agent solutions within an injection molding machine. Polymer Engineering and Science 45, 2005, 1108-1118.

[30] Gornik C. Determining rheological data directly at the machine. Kunststoffe Plast Europe 4, 2005, 88-92.

[31] Kelly AL, Gough T, Whiteside BR, Coates PD. High shear strain rate rheometry of polymer melts. Journal of Applied Polymer Science 114, 2009, 864-873.

[32] Haddout A, Villoutreix G. Polymer melt rheology at high shear rates. International Polymer Processing XV(3), 2000, 291-296.

[33] Benhadou M, Haddout A. Injection of polypropylene reinforced with short glass fibers: Rheological behavior. Journal of Reinforced Plastics and Composites 26(13), 2007, 1357-1366.

[34] Mobuchon C, Carreau PJ, Heuzey M-C, Sepehr M. Shear and extensional properties of short glass fiber reinforced polypropylene. Polymer composites, 2005, 247-264.

[35] Sentmanat M. Miniature universal testing platform: from extensional melt rheology to solid-state deformation behavior. Rheologica Acta 48, 2004, 657-669.

[36] Franck A, The ARES-EVF: Option for measuring extensional viscosity of polymer melts.
Available from
http://www.tainstruments.com/pdf/literature/APN002_V2_ARES_EVF_to_measure_elongation_viscosity.pdf. Accessed 2010 Sept 28.

[37] Padmanabhan M, Kasehagen LJ, Macosko C. Transient extensional viscosity from a rotational shear rheometer using fiber-windup technique. Journal of Rheology, 40, 1996, 473-481.

[38] Svrcinova P, Kharlamov A, Filip P. On the measurement of elongational viscosity of polyethylene materials. Acta Technica 54, 2009, 49-67.

[39] Soulages JM, McKinley GH, Hall NR, Magee KS, Chamitoff GE, Fincke ME. Characterization of a dilute polymer solution following preshear in microgravity. Society of Rheology Annual Meeting 2009, Madison, WI, USA, Book of Abstracts, 75.

[40] SER universal testing platform. Available from http://www.xpansioninstruments.com/images/SER2_Literature.pdf. Accessed 2010 Dec 07

[41] Lyhne A, Rasmussen HK, Hassager O. Simulation of elastic rupture in extension of entangled monodisperse polymer melts. Physics Review Letters 102, 2009, 138301-1 – 1383101- 4.

[42] Meissner J, HostettlerJ. A new elongational rheometer for polymer melts and other highly viscoelastic liquids. Rheologica Acta 33, 1994, 1-21.

[43] Münstedt H. New universal extensional rheometer for polymer melts. Measurements on a polystyrene sample. Journal of Rheology, 23, 1979, 421-436.

[44] Bach A, Rasmussen HK, Hassager O. Extensional viscosity for polymer melts measured in the filament stretching rheometer. Journal of Rheology 47, 2003, 429-441.

[45] Meissner J. Dehnunhgsverhalten von Polyetylen-Schmelzen. Rheologica Acta 10,1971, 230-240.

[46] Tsenoglou CJ, Voyiatzis E, Gotsis AD. Simple constitutive modeling of nonlinear viscoelasticity under general extension. Journal of non-Newtonian Fluid Mechanics 138, 2006, 33-43.

[47] Wagner MH, Bernnat A. The rheology of the Rheotens test. Journal of Rheology 42, 1998, 917-928.

[48] Kaschta J, Münstedt H. Measuring the elongational properties of polymer melts – A simple task? Conference proceedings The XVth International Congress on Rheology, 2008, 1105-1107.

[49] Rides M, Allen CRG, Chakravorty S. Intercomparison of extensional flow characterization techniques for polymer melts: tensile stretching and converging flow methods. Report CMMT(A)171, Centre for Material Measurement and Technology, National Physics Laboratory, Teddington, Middlesex, UK, 1999.

[50] Rides M. Draft ISO Standard for the determination of the transient extensional viscosity of polymer melts. Report CMMT(A)248, Centre for Material Measurement and Technology, National Physics Laboratory, Teddington, Middlesex, UK, 2000.

[51] Kalika DS, Nuel L, Denn MM. Gap-dependence of the viscosity of a thermotropic liquid crystalline copolymer. Journal of Rheology 33, 1989, 1059-1070.

[52] Rosato DV, Rosato DV, Rosato MG, Eds. Injection molding handbook. 3rd Ed. Dordrecht: Kluwer Academic Publishers; 2000. 1485 p.

[53] Mitsoulis E. Effect of viscoelasticity in fountain flow of polyethylene melts. International Polymer Processing XXIV(5), 2009, 439-451.

[54] Mnekbi C, Vincent M, Agassant JF. Polymer rheology at high shear rate for microinjection moulding. International Journal of Material Forming, 3, 2010, 539-542.

[55] Kelly AL, Gough T, Whiteside BR, Coates PD. High shear strain rate rheometry of polymer melts. Journal of Applied Polymer Science 114, 2009, 864-873.

[56] Mitsoulis E, Hatzikiriakos SG. Bagley correction: the effect of contraction angle and its prediction. Rheologica Acta, 42, 2003, 309-320.

[57] Binding DM, Couch MA, Walters K. The pressure dependence of the shear and elongational properties of polymer melts. Journal of Non-Newtonian Fluid Mechanics, 79, 1998, 137-155.

[58] Kennedy PK. Practical and scientific aspects of injection molding simulation. PhD Thesis, Technishe Universiteit Eindhoven, The Netherlands, 2008.

[59] Osswald T, Hernández-Ortiz JP. Polymer processing – Modeling and simulation. Munich; Carl Hanser Verlag, 2009, 606 p.

[60] Cardozo D. A brief history of the filling simulation of injection moulding. Journal of Mechanical Engineering Science, 223, 2009, 711-721.

[61] Hieber CA, Shen SF. A finite element/ finite difference simulation of the injection-molding filling process. Journal of Non-Newtonian Fluid Mechanics 7, 1980, 1-32.

[62] Ray S. A three-dimensional flow simulation using a viscoelastic constitutive equation and a segregated finite element scheme. PhD Thesis, Swinburne University of Technology, Australia, 2000.

[63] Papathanasiou TD, Kamal MR. Filling of a complex-shaped mold with a viscoelastic polymer. Part I: The mathematical model. Polymer Engineering and Science, 33(7), 1993, 410-417.

[64] Kamal MR, Papathanasiou TD. Filling of a complex-shaped mold with a viscoelastic polymer. Part II: Comparison with experimental data. Polymer Engineering and Science, 33(7), 1993, 400-409.

[65] Bogaerds ACB, Hulsen MA, Peters GWM, Baaijens PT. Stability analysis of injection molding flows. Journal of Rheology, 48(4), 2004, 765-785.

[66] Kwon K, Isayev AI, Kim KH. Toward a viscoelastic modeling of anisotropic shrinkage in injection molding of amorphous polymers. Journal of Applied Polymer Science, 98, 2005, 2300-2313.

[67] Cao W, Shen C, Zhang C, Wang L. Computing flow-induced stresses of injection molding based on the Phan-Thien-Tanner model. Archives of Applied Mechanics, 78, 2008, 363-377.

[68] Brincat P, Talwar K, Friedl C. Extensional viscosity modeling for injection molding simulation. Journal of Reinforced Plastics and Composites 18(6), 1999, 499-507.

[69] Speight RG, Costa F, Kennedy PK, Friedl C. Best practice for benchmarking injection molding simulation. Plastics Rubbers and Composites 37, 2008, 124-130.

[70] Sherbelis G, Friedl C. The importance if pressure dependent viscosity and contraction pressure losses to injection molding CAE analysis. SPE ANTEC Technical Papers, 1996, 778-782.

[71] Cadmould 3D-F product information. Available from http://www.simcon-worldwide.com/pages/en/products/cadmould.php. Accessed 2010 Aug 25.

[72] Autodesk Moldflow Insight product information. Available from http://usa.autodesk.com/adsk/servlet/pc/index?id=12269104&siteID=123112. Accessed 2010 Aug 25.

[73] Huilier DFG. Modeling of injection mold post-filling: a review and some critical problems to solve. Journal of Polymer Engineering, 9(4), 1990, 237-302.

[74] Gupta M. Estimation of elongational viscosity of polymers for from entrance loss data using individual parameter optimization. Advances in Polymer Technology 21(2), 2002, 98-107.

[75] Moller JC, Lee D. Verification of extensional viscosity effects in injection mold filling simulation. Polymer Engineering and Science, 42(2), 2002, 307-325.

[76] Perera SSN. Sensitivity of viscoelastic melt spinning processes with respect to operating conditions and material constants. Nihon Reoroji Gakkaishi (Journal of the Society of Rheology, Japan) 37(3), 2009, 143-147.

[77] Fourné F. Synthetic fibers – Machines and equipment, manufacture, properties. Handbook for plant engineering, machine design, and operation. Munich: Hanser Publishers; 1998. 930 p.

[78] Ivanov, I, Muke S, Kao N, Bhattacharya SN. Extensional rheology of polypropylene in relation to processing characteristics. International Polymer Processing XIX(1), 2004, 40-46.

[79] Lee JS, Jung, HW, Hyun JC. Frequency response of film casting process. Korea-Australia Rheology Journal, 15(2), 2003, 91-96

[80] Lee S, Kim BM, Hyun JC. Dichotomous behavior of polymer melts in isothermal melt spinning. Korean Journal of Chemical Engineering 12(3), 1995, 345-351.

[81] Laffargue J, Demay Y, Agassant JF. Investigation of polymer stretching instabilities: Application to film blowing, International Polymer Processing XXV(5), 2010, 356-371.

[82] Steffl T. Rheological and film blowing properties of various low density polyethylenes and their blends. PhD Thesis, University of Erlangen-Nürnberg, Germany, 2004.

[83] Takahashi H, Matsuoka T, Kurauchi T. Rheology of polymer melts in high shear rate. Journal of Applied Polymer Science 30, 1985, 4669-4684.

[84] Takahashi H, Matsuoka T, Ohta T, Fukumori K, Kurauchi T, Kamigaito O. Rheological behaviour of SAN/PC blends under extremely high shear rate. Journal of Applied Polymer Science 37, 1989, 1837-1853.

[85] Janeschitz-Kriegl H. How to understand nucleation in crystallizing polymer melts under real processing conditions. Colloid and Polymer Science 281, 2003, 1157-1171.

[86] Janeschitz-Kriegl H, Eder G, Stadtlbauer M, Ratajski E. A thermodynamic frame for the kinetics of polymer crystallization under processing conditions. Monatshefte für Chemie 136, 2005, 1119-1137.

[87] Bastian H. Non-linear viscoelasticity of linear and long-chain-branched polymer melts in shear and extensional flows. PhD Thesis, University of Stuttgart, Germany, 2001.

[88] Wagner MH, Rubio P, Bastian H. The molecular stress function model for polydisperse polymer melts with dissipation convective constraint release. Journal of Rheology 45, 2001, 1387-1412.

[89] Wagner MH, Yamaguchi M, Takahashi M. Quantitative assessment of strain hardening of low-density polyethylene melts by the molecular stress function model. Journal of Rheology, 47, 2003, 779-793.